Michigan State University

National Superconducting Cyclotron Laboratory

PRELIMINARY DESIGN STUDY EXPLORING BUILDING FEATURES REQUIRED FOR A PROTON THERAPY FACILITY FOR THE ONTARIO CANCER INSTITUTE

H. BLOSSER, D. JOHNSON, D. LAWTON, R. RONNINGEN
R. BURLEIGH, and B. GOTTSCHALK

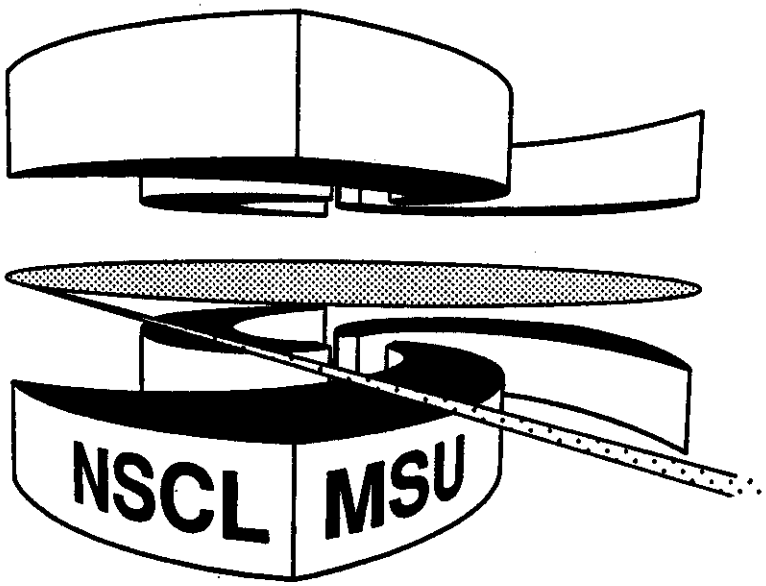

MSUCL-760a

MARCH 1991

PRELIMINARY DESIGN STUDY

EXPLORING

BUILDING FEATURES REQUIRED

FOR A

PROTON THERAPY FACILITY

FOR

THE ONTARIO CANCER INSTITUTE*

H. BLOSSER, D. JOHNSON, D. LAWTON, R. RONNINCEN & R. BURLEIGH

NATIONAL SUPERCONDUCTING CYCLOTRON LABORATORY**
SOUTH SHAW LANE
MICHIGAN STATE UNIVERSITY
EAST LANSING, MICHIGAN, 48823 USA

&

B. GOTTSCHALK

HARVARD CYCLOTRON LABORATORY
44 OXFORD ST..
CAMBRIDGE, MASSACHUSETTS 02138, USA

MSUCL-760a

MARCH 1991

* Site specific studies supported by Ontario Cancer Institute; basic research studies supported by the US National Science Foundation, Michigan State University, and the Harvard Cyclotron Laboratory.

** A national nuclear physics user facility operated by the US National Science Foundation under Cooperative Agreement PHY-8913815.

CONTENTS

I. INTRODUCTORY REMARKS

The object of the work described in this report is to provide background information to allow development at the Princess Margaret Hospital (Ontario Cancer Institute, Toronto, Ontario M4X 1K9) of an architectural plan for a new hospital structure that will include areas configured for later installation of an accelerator and treatment room system appropriate for cancer radiation therapy using beams of high energy protons as the therapeutic agent. Such beams are presently used for cancer therapy at two centers in the US (Massachusetts General Hospital and Loma Linda University Medical Center) and at approximately ten centers in Europe and Japan. The facility envisaged in this study would provide proton therapy capability in the Province of Ontario.

A proton therapy facility requires a particle accelerator capable of generating proton beams in the 220 to 250 MeV (million electron volt) energy range, and a beam transport system to distribute the proton beam(s) to one or more treatment rooms. If desired, the treatment room can include an isocentric beam delivery system (a "gantry") so that the beam can be directed at the patient from any desired direction, as is standard in modern X-ray radiation therapy facilities. From the architectural perspective, the treatment rooms are typically the dominant aspect of a proton therapy facility and the detailed design of the gantry is in turn the dominant architectural feature of the treatment room. At present (Jan. 1991) gantries actually exist in only one of the operating proton therapy facilities (Loma Linda) and even in that facility the gantry has not yet been brought online as an active patient treatment facility. Actual experience with a gantry system for proton therapy is then not available at this time and experience with neutron therapy gantries at a number of medical centers is only partially relevant. The great size of the Loma Linda gantries (11 meters in diameter -- written hereafter 11m or 11,000mm, etc.) has led to many suggestions for alternate more compact gantry structures, and the elegant $400M heavy ion facility under construction at Chiba in Japan has elected not to provide gantries, but rather to use fixed vertical and horizontal beams. Noting the architectural dominance of the gantry issue, the first part of this report reviews issues involved in the design of the treatment room(s) and particularly features which impact the gantry decision.

After the treatment rooms, the next most important architectural feature of a proton therapy facility is the accelerator room. The accelerators used in older proton therapy facilities are almost all synchrocyclotrons (also known as frequency modulated, or "fm", cyclotrons) and all of these cyclotrons use room temperature magnets. The most recently constructed facility (at Loma Linda) on the other hand uses a proton synchrotron as the primary accelerator, and superconducting synchrocylotrons, and room temperature and superconducting isochronous cyclotrons all have attractive features relative to the traditional room temperature synchrocyclotron, and all have been studied in various degrees as possible candidate accelerator systems for a modern proton therapy facility. Section III of this report reviews the relative advantages of these alternatives in the envisaged Princess Margaret Hospital situation.

One of the likely accelerator choices, a superconducting isochronous cyclotron, has not heretofore been explored in a comparable degree to the other accelerator systems. Recent studies at MSU have therefore focused on more detailed development of design features of an accelerator system of this

type. Some of the important results of these studies are presented in Section IV.

Section V of this report presents a number of possible specific plans for a proton therapy facility at Princess Margaret Hospital (PMH). The layouts selected match reasonably with the already far advanced architectural planning of the new PMH building. Technical assumptions and technical uncertainties of each arrangement are outlined and the further studies which would be required to firmly establish the feasibility of each configuration are described. The section also includes a tabulation of utilities requirements and space for utilities for the various options.

The final section of this report presents a "Suggested Work Plan" for proceeding further with planning of a modern proton therapy facility for Princess Margaret Hospital.

II. TREATMENT ROOM FACTORS

Three major factors enter into the determination of the overall size of the treatment rooms, namely:

1. Will the facility include a continuously variable isocentric beam system (a gantry)?
2. What are largest radiation fields which will be used in the facility? and,
3. How strong are the magnets which will be used to bend the beam?

This report will largely pass over the no-gantry option since most groups involved in planning new heavy particle therapy facilities have decided that a gantry is a medically very important capability which should therefore be provided in a new facility. (The exception to this, the Japanese facility at Chiba, is primarily a heavy ion facility; such beams are much more rigid than a therapy proton beam and a gantry would therefore need to be considerably larger than that required for protons.) The possible architectural plans given in section V of this report include one no-gantry system similar to the configuration under construction at Chiba.

A. BEAM SPREADING

Typically the most significant space requirement in a gantry based therapy system arises from the need to spread the beam over the area and depth of the desired treatment volume. The beam as it emerges from the accelerator is small compared to the size of all but the smallest tumors and a system for spreading the beam to the desired size is needed. This system must moreover distribute the beam in a uniform way so that subsections of the target volume are neither underdosed nor overdosed.

Figure I is a schematic drawing showing essential features of a treatment plan for proton irradiation. The target volume exists at a depth within the patient and has both a thickness and a transverse size which are usually large compared to the intrinsic distribution of the beam. The beam must therefore be spread in both the transverse plane and in depth to accomplish the desired treatment.

Spreading the beam in depth is accomplished by shifting the energy of the proton beam so that the intrinsic sharpness of the "Bragg peak" associated

with monoenergetic protons is converted into a "spreadout" Bragg peak [1] with the flat region matching the thickness of the treatment volume in the depth coordinate, as is shown schematically in Figure II. In principle the spread in depth can be accomplished by varying the energy of the accelerator, but even for accelerators with easily variable energy, such as synchrotrons, it is technically rather difficult to vary magnet strengths throughout the beam transport system without introducing unwanted transverse beam displacements. Thus, at this time, the technique of choice for spreading the beam in depth is to insert a range "modulator" i.e. a device usually in the form of a wheel with spokes of varying thickness through which the beam must pass, the thickness of each spoke selected to give the degree of energy reduction needed to shift the beam range to the successive layers needed for the desired degree of flattening, as illustrated in Figure II.

The schematic target volume in Figure I shows a curving "distal edge" (the surface of the target volume opposite to the point of beam entry into the tumor) as is typical in an actual therapy situation. To accommodate treatment fields with such curving distal surfaces, a customized range compensator called a "bolus" is introduced just in front of the patient so that the total proton energy loss from the front edge of the bolus to the distal edge of the target volume is the same at all points of the target, i.e. the bolus is thin at points where the distal edge of the target volume is deep within the patient and is thicker at locations where the distal edge of the volume to be treated is closer to the skin.

The system most widely used for transverse beam spreading at the present time was developed at Harvard and makes use of the scattering of the beam as it passes through thin solid foils (e.g. lead). Such scattering yields a roughly Gaussian distribution in angle for the protons emerging from the scatterer, which becomes a Gaussian distribution in radius by the time the protons reach the isocenter. With just one scatterer, only the very central portion of the Gaussian is flat enough to be useful. Therefore only a small fraction of the beam is used and even then, the energy loss in the relatively thick scatterer is considerable, leaving less range available in the patient. The Harvard scheme [2] overcomes this by using two scatterers, the first a simple lead foil and the second, a lead foil partly blocked by a cylindrical brass annulus as shown in Figure III. The annulus creates a hole in the Gaussian which is subsequently filled in by the action of the second scatterer. In a well-optimized system 30% of the incident protons reach the flat dose region where the dose uniformity can be as good as ±2.5%, and the lead foils are thin so that only a few mm of range in water need be lost. The range modulator and a variable absorber to adjust penetration are placed downstream fairly near the patient. This arrangement has the advantage of allowing transverse spreading and depth spreading to be handled separately, but the modulator/absorber in its downstream location introduces an unwanted third scatterer which degrades the penumbra of the proton beam.

During the past two years several improvements have been introduced in the Harvard system [3]. First, as shown in Figure IV, the modulator is placed upstream at the beginning of the beam spreading system so that it doubles as the first scatterer. This allows it to be small (hence rotate rapidly) and more importantly, gets rid of the "third scatterer" effect mentioned above. Second, the "annulus" style second scatterer is replaced by a "contoured scatterer", so that the Gaussian from the first scatterer is flattened by scattering it more strongly at the thicker central part of the contoured scatterer. With this system, total proton losses are down so that 46%

efficiency can be achieved, and the system is less sensitive to beam steering. The unequal energy loss at different radii is compensated by a contoured plastic plate. The only disadvantage relative to the annulus is somewhat greater energy loss since more lead is needed at the center. Such beam spreading systems (with upstream modulator and contoured scatterer) have been built and tested at Harvard. They show good agreement with predictions, and are currently being integrated into the therapy program.

Anticipating that later sections will establish a 220 MeV accelerator with approximately 2 meters of drift space, or "throw", between the last magnetic element and the patient as likely Princess Margaret Hospital parameters, and that a field diameter of at least 15 cm is needed, a new Harvard computer program [4] has been used to develop a reference design for a state-of-the-art scattering system to spread the beam to this specification. The parameter set for the computer calculation is given in Figure V-A. The results of the calculation show that a 20 cm diameter field can be treated with the 220 MeV beam up to a depth in water of 25 cm. Fig. V-B shows schematic representations of the modulator and contoured scatterer, a depth-dose distribution and transverse distributions at three depths, using as input a Bragg peak measured with the Loma Linda synchrotron. The design has not been highly optimized but even so, the dose is within the ±2.5% tolerance everywhere.

Any passive scattering system allows tradeoffs (by redesigning the components) between treatment depth, field diameter, throw, and incident energy. For instance, if a larger diameter is to be treated, thicker scatterers are required and the maximum depth (given constant throw and energy) is therefore reduced. The easiest way to summarize all the possibilities is to start with a reasonable reference design e.g. Fig. V and give the first order formula relating changes in D the maximum treatment depth (cm H_2O), L the throw (m), T the incident energy (MeV) and R the radius of uniform dose (cm). The design program [4] can be used to compute the numerical coefficients, and for the Fig. V system the formula is:

$$\Delta D = 3.41\Delta L + 0.196\ \Delta T - 0.983\ \Delta R$$

where Δ stands for the change in the corresponding quantity. This formula is accurate even for fairly large Δ's. For instance if energy and throw are not changed but we wish a 30 cm diameter field (R greater by 5 cm, $\Delta R = +5$) the formula predicts that D will decrease by 5 cm, whereas an actual redesign gives $\Delta D = -5.3$cm.

In summary, the disadvantages of a scattering system for spreading the beam are:

1. A relatively long flight path (or throw) is required from the first scatterer to the patient and this flight path follows the last bending magnet so that it becomes the dominant element in determining gantry size. (The Loma-Linda gantry provides 3.5 meters from the exit of the last bending magnet to the isocenter.)
2. When larger fields are used, the needed scatterer thickness reduces the beam energy and therefore the penetration depth, as is shown in Figure V for a system where the first scatterer is 2.25 meters from the distal edge of the treatment volume.
3. The beam is approximately an expanding irregular cone from the first scatterer to its final depth and as this cone expands within the

patient the dose falls off since a given number of particles are spread over a larger area. This fall off is compensated in the modulator design program which calculates a 'sloping top' on the spreadout Bragg peak to give a net dose vs. depth which is flat. The conical edges of the treatment volume defined by the first scatterer and the patient aperture however remain as a constraint. In extreme situations (scatterer closein and treatment volume extending from shallow to deep) the dose at the skin can exceed the dose at depth and become the limiting factor in one portal treatment plans [5].

In comparison with these disadvantages, a scattering system has two very compelling advantages, namely, simplicity and reliability. As a consequence, scattering remains at the present time the system of choice even though much attention has been devoted to conceptional studies of alternate systems which match the proton distribution more efficiently to the desired target volume and which allow more compact gantry structures.

If scattering is designated as a passive beam spreading system (no time varying elements except for the rotating modulator wheel which is quite reliable), active systems in approximately ascending order of complexity include:

1. Using a "wobbler" magnet to swing the beam in an annular path about its central axis, thereby accomplishing the same effect as the scattering foil but without energy loss (a technique employed in the heavy ion therapy program at Lawrence Berkeley Laboratory [9]).

2. Forming the beam into a line image in the transverse plane with the length of the line set by a slit system and with the other transverse coordinate scanned by moving the patient (much like the system used in the pion therapy system at PSI [6]).

3. Provide spreading in one transverse coordinate by using a magnet prior to the last bend to sweep the beam left and right relative to the bending plane of the last magnet so that a wider aperture in this magnet will transmit the full beam. Spreading in the perpendicular coordinate can be provided by either motion of the patient or by a slight rotation of the last magnet about the axis defined by the initial entering beam (a system suggested by Jongen of IBA [7]). A related system in which the beam sweeps in both transverse directions has been studied by Enge [8]; in this situation the aperture of the last magnet must be enlarged in both height and width in order to transmit the expanding beam.

4. Using either a pixel or raster scanning system to move the beam rapidly back and forth in one transverse coordinate accompanied by a slower transverse motion in the perpendicular coordinate in the fashion of the electron beam in a TV tube. If the system includes a fast on/off capability, the transverse edges of the treatment volume could be set by using the on/off trigger and the projected cone constraint in the depth plane could then be released giving the option of size vs. depth profiles which more closely match the actual tumor shape. (Systems of this type, in the aspect of using a very concentrated beam, involve a challenging safety requirement in the need to insure that the beam is quickly turned off in the event the scanning motion is inadvertently interrupted [such as an electrical spark in the scanning system might cause]; if such a concentrated beam is left stationery it can quickly deliver a lethal does to the affected tissue similar in effect to the penetration of a bullet.)

As the discussion already makes clear, the features of the beam spreading system, in many (or most) situations interact with and must match related features of the gantry system, the primary goal of most of the alternate beam spreading system proposals being to allow use of smaller gantries, as is discussed in the next sub-section. A second important beam spreading system

goal is more efficient use of the proton beam -- even if the accelerator can provide more than enough intensity, protons which fail to reach the treatment volume produce unwanted prompt radiation and unwanted residual radioactivity, and reducing these components is always desirable.

B. GANTRY SYSTEMS

Several possible gantry/beam spreading configurations are shown in Figures VI, VII and VIII. Figure VI, which is taken from ref. [8] , first of all shows three structures considered in a study at Harvard. The "classic" gantry in the center and the "corkscrew" gantry on the right are sized to provide a 4m space from the last magnet to the isocenter which comfortably provides space for scattering or wobbling the beam, or for pixel or raster scanning. The "Enge" system, on the left in the Figure, as discussed in the previous sub-section, sweeps the beam in both transverse directions prior to entering the large gantry magnets which therefore need to have an expanding aperture in both coordinates to transmit the expanding beam. The IBA gantry [7] shown in Figure VII is similar to the Enge gantry in the aspect of sweeping the beam before the last bending magnet but the sweep in the IBA system is in only one coordinate and the perpendicular direction is provided by rotating the magnet through a small angle as indicated by the circular arrow at the upper right of the Figure. Figure VIII shows still another gantry arrangement developed at MSU by Sherrill [10] -- in this structure the beam is focused to a "line" as indicated by the "Transport" output at the bottom of the Figure, the line being 1cm in transverse width in the plane of the bending magnets and 30cm in the perpendicular coordinate -- the line is moved through the tumor with a sweeping magnet near the patient or the patient is moved relative to the line by appropriate programming of the patient table drive (as in the pion therapy system at PSI [6]).

One important feature of a gantry system is the total angle of bending. Referring to Figure VI, it's clear that the total bending angle for the Enge system is 90° less than that of the classic gantry which is in turn 90° less than the bending in the corkscrew gantry (the latter not directly clear in the Figure -- the magnet at the top is a 135° bend in the plane perpendicular to the isocentric axis followed further on by a second 135° bend in the same plane which directs the beam back to the axis). Since magnets are one of the major cost elements of a gantry, structures with large total bend tend to be higher in cost. Magnet aperture is another sensitive cost factor, the large two dimensional aperture of the Enge magnets being a disadvantage in this regard, and the large one dimensional aperture of the IBA magnets also disadvantaged but to a lesser degree. A classic gantry can also be arranged in the 45°, 45°, 90° sequence used in the Enge gantry to give a 180° total bend but with more space required than for the classic gantry shown in Figure VI.

The major attractive feature of the corkscrew gantry is reduced space in the longitudinal direction and this is the configuration which is used in the Loma Linda facility. Shielding walls might also be reduced by putting shielding for the gantry slot onto the gantry (so that it rotates with the magnet system). The corkscrew system involves bending the beam in perpendicular planes which is a more exacting control problem than when bends are all in one plane (in the latter a bending error in one magnet can be corrected by an offsetting bend in nearly any other magnet -- if more than one bending plane is used each plane must be separately corrected). The corkscrew gantry on the other hand involves a magnet spacing which easily allows an

achromatic beam transport condition to be imposed [22], and this is very helpful in reducing the sensitivity to the beam energy spread and to beam energy fluctuations. The 45° bending section of a corkscrew gantry also acts to crowd the region near the patient as can be seen in the actual mechanical layout of the Loma Linda gantry [11] shown in Figure IX, where the clearance between the isocenter and the 45° line is seen to be just 1.4m (4.6'). (This comparison is conjectural in the aspect that equivalent mechanical layouts for other gantry systems have not yet been made; actual clearances for such systems may well be sizably smaller than is presently apparent when realistic mechanical support systems are included.)

Most of the gantry alternatives proposed by various workers have not as yet been fully designed. For some proposals, only bending angle layouts have been made, others have progressed to include optical calculations of focusing effects for ideal magnets, and, for the Loma Linda gantry, actual construction details of the magnets have been developed, the magnets have been built, and performance results are beginning to be available.

Considering the Princess Margaret Hospital situation, space limitations in the already well advanced architectural planning at Princess Margaret Hospital make a direct copy of the Loma Linda gantry design impractical. The extensive effort involved in fully exploring any single gantry design means that effort will need to be focused on one or a few options selected somewhat intuitively as being well matched to the PMH boundary conditions. The initial intuitive choices should involve PMH physics and medical staff as well as consultants since these choices will have an extremely important impact on the overall long range effectiveness of the final facility.

C. MAGNET STRENGTH

After the beam spreading system (or more explicitly the distance from the last magnet to the isocenter), the next most important parameter effecting the overall size of the gantry is the bending radius of the beam in the magnets. The beam energy determines the product of magnetic field strength and radius -- for 220 MeV protons this product is 2.26 Tesla-meters (Tm) and for 250 MeV the product is 2.43Tm. The electric energy consumed by normal iron and copper magnets operating at room temperature leads to excessive cost as the field strength approaches 2T, and the gantry magnets at Loma Linda operate at 1.6T which is a well optimized design strength. The resulting bending radius (1.41m for 220 MeV and 1.52m for 250 MeV) is however large relative to the space available at Princess Margaret; this then provides a strong incentive to increase the field strength in the bending magnets to obtain tighter beam bends and thereby reduce the overall size of the gantry. Some interesting field strengths to consider are 2.25T, more-or-less the extreme limit of room temperature magnets, 3.5T, an easy superconducting field strength which at the same time leaves adequate room for iron to contain the stray magnetic field, and 5.0T, a normal field strength for superconducting magnets but with considerable stray field. These three choices then give beam radii (at 220 MeV) of 1.0m, .65m, and .45m respectively and the gantry diameter relative to 1.6T is reduced by .82m, 1.52m, and 1.92m respectively. The secondary role of bending radius relative to the isocenter spacing is evident from comparing these reductions to the 11m total diameter of the Loma Linda gantry; changes which move the beam spreading system ahead of the last bending magnet (the Enge design, the IBA design, the MSU design, etc.) reduce gantry diameter by 2 to 4m and are therefore the initial focus of smaller gantry studies. Combining a compact type gantry with a moderate field enhancement in the

gantry magnets (to say 3.5T) may well give the most attractive overall package, and particularly so in the circumstance where the accelerator system is also superconducting, so that a liquid helium system would already be included in the facility configuration.

III. ACCELERATOR CONSIDERATIONS

Accelerators which operate in the 200 MeV energy range include linacs, synchrotrons, synchrocyclotrons, and isochronous cyclotrons and all of these can be either room temperature or superconducting. Of these, the linac has usually been quickly eliminated as too costly, although recent work at Los Alamos [12] is trying to address this disadvantage. For the Princess Margaret situation, the length of a linac is also a problem, and so this option has not been considered further.

The accelerator used at the Loma Linda proton therapy facility is a synchrotron and the size is such that it can be snugly fitted into a room which is 24 feet by 24 feet, a size which is just feasible in the Princess Margaret situation. (Some additional length would be required if treatment rooms are to go on two sides of the accelerator, so that three electron accelerator bays would probably have to be deleted -- the accelerator and one treatment room would fit in a two bay space.) From the accelerator perspective, the synchrotron is intrinsically more complicated than either an isochronous or a synchro-cyclotron but it has an important advantage in its ability to easily produce any energy up to the maximum. Variable energy in a cyclotron is possible and is a standard feature of all recent nuclear research cyclotrons, but complicated additions to the cyclotron structure are needed which would add 50 to 60% to the cost of the cyclotron.

With respect to intensity, the beam from the synchrotron at Loma Linda is less intense than expected and large field treatments will take longer than had been hoped. A higher energy injector or faster cycling of the magnets would however readily correct this problem and either of these features could easily be included in a second generation machine. The Loma Linda synchrotron also has the important advantage of being offered for sale by a commercial company [13] on a fixed price basis, and, since a first such accelerator is in operation, the level of technical risk in this option is clearly lower than for other suggested systems. The principal disadvantage of the synchrotron from the Princess Margaret perspective is its size. If a more detailed exploration of this option is of interest, the commercial vendor would probably be willing to undertake planning studies.

The several cyclotron options (synchro- or isochronous, room temperature or superconducting) have much in common in terms of basic structure, i.e. a large magnet, an rf system, an ion source, an extraction system, etc. One important distinguishing feature is the weight and size of the magnet which for given energy decreases as the field strength is increased. As with gantry magnets, cost considerations make superconducting systems the design of choice for field strengths above 2T, but focusing limits the field strength to 3T if the system is isochronous. Approximately, the magnet weight of a 220 MeV proton cyclotron would be 55 tonnes for a 5T synchrocyclotron, 80 tonnes for a 3T isochronous cyclotron (both superconducting) and 180 tonnes for a 2T room temperature isochronous cyclotron. (These weights seem large but from the aspect of building construction are not unusual; a shielding wall 2m thick, 10m long and 8m high for comparison weighs about 370 tonnes.)

Light weight designs are particularly helpful in systems where the accelerator is rotated with the gantry; if the whole system rotates as the beam is shifted to different angles, all beam bends are in one plane, a feature which considerably simplifies tuning of the beam (as mentioned previously in the discussion comparing conventional and corkscrew gantries). A rotating accelerator is clearly more complicated to construct than a fixed accelerator but the needed technology has been developed for the neutron therapy accelerator at Harper Hospital [14]. In this facility a 22 tonne superconducting cyclotron rotates on a full 360° trajectory about a supine patient; the total rotating mass is approximately 55 tonnes. Either a 55 tonne or an 80 tonne cyclotron could certainly be rotated with a very similar system and a 180 tonne cyclotron could undoubtedly also be rotated although the extrapolation from existing technology is considerably larger. A very difficult issue to resolve is the question of whether it is better to choose a rotating accelerator design, thereby adding complexity to the construction of the facility in order to have the later benefit of simplified operation vs. a fixed accelerator which has the reverse characteristics. Clearly most experts presently involved in the planning of proton therapy facilities opt for the fixed accelerator approach and this body of opinion should not be lightly overlooked; most of these experts are however to a significant degree influenced by the technical difficulty of rotating the accelerator and few have personally observed the operation of the Harper system; observing this accelerator adds an intuitive backup to the assertion that the rotation technology exists.

Isochronous and synchro-cyclotrons differ principally in the acceleration systems, the isochronous cyclotron using a relatively high voltage CW (constant wave) system and the synchrocyclotron using a frequency modulated lower voltage system. Both of these accelerators use a magnetic field which is constant in time, rather than varying with time as in the synchrotron; in the isochronous cyclotron the shape of the magnetic field is stringently constrained in comparison to the shape requirements for a synchrocyclotron, but techniques for achieving the required tolerances are well developed. Relative to the synchrocyclotron, an isochronous cyclotron would typically be more expensive by perhaps 50% and give higher beam current by perhaps one hundred fold. Both accelerators are capable of delivering much higher beams than are needed for therapy, 0.02 microamps being widely viewed as the needed therapy current whereas 1 and 100 microamps would be normal currents for synchro- and isochronous cyclotrons respectively. A recent innovation in the Harper Hospital cyclotron blurs the line of separation between the synchro- and isochronous cyclotron by pulsing the CW rf of the isochronous cyclotron; this lowers the required rf power and the current is still more than adequate as a consequence of the large excess intrinsic current capability of isochronous cyclotrons.

A rather unusual difficulty which arises in the synchrocyclotron situation is the fact that the technology is to a considerable degree forgotten, it being now many years since such a cyclotron was constructed. A special sensitive area where new R&D should be pursued is in the system which modulates the frequency; greatly improved frequency modulation techniques have been developed since synchrocyclotrons were last constructed but the step of adapting this technology to the synchrocyclotron situation needs to be worked out.

Considering the various relevant factors -- cost, reliability, compactness, predictability, compatibility with rotation,... -- a likely

ranking of accelerator attractiveness vs. Princess Margaret constraints would seem to be:

1) 3T superconducting isochronous cyclotron,
2) 2T room temperature isochronous cyclotron,
3) Loma Linda style synchrotron,

with other options significantly less attractive.

IV. DESIGN FEATURES OF 3 TESLA ISOCHRONOUS CYCLOTRON

Of the accelerator systems considered in the previous section, the 3T isochronous cyclotron had attractive features relative to other options but, at the beginning of this study, was the least explored in terms of actual technical design of the accelerator. In view of this an initial exploration of detailed technical features of such an accelerator was undertaken.

A basic plan view of such a cyclotron is given in Figure X. The outer yoke is cylindrical as in most superconducting cyclotrons, in order to maximize magnetic efficiency and reduce external magnetic fields. The superconducting coil is housed in an insulating vacuum separate from the main acceleration chamber vacuum, so that the coil can stay at cryogenic temperatures while occasional maintenance work is performed in the beam chamber. (The superconducting coil of the MSU K500 cyclotron, the oldest of the superconducting cyclotrons, was last warmed to room temperature in 1982 [15].) The cyclotron magnet is a "4 sector" design, i.e. the hill and valley structure which provides axial focusing repeats four times, and the hills and valleys are also strongly spiraled which further strengthens the focusing. The accelerating electrodes ("dees") are located in the valleys of the magnet and are also strongly spiraled. Figure XI is a section view of the magnet showing the superconducting coil in cross section, and the hill and valley gaps on the right and left of the central axis. Figure XII is a section view perpendicular to the central spiral line of the dee and shows the dee stem structure needed in order to have a high "Q" structure resonating at 37.3 Mhz, the required isochronous frequency.

For nearly cylindrical high field magnets, codes exist which predict the magnetic field shape with adequate accuracy. Figure XIII is a contour map of the results of such a calculation for a magnet of the form shown in the previous Figures. Figure XIV shows the azimuthal average of the magnetic field from Figure XIII, the solid line, vs. the value needed for isochronous operation. The two curves are in good agreement considering the preliminary state of the design, and can clearly in later stages of the design be brought to the needed 1 in 10,000 agreement by small adjustments in the shape of the pole tips. Since the cyclotron energy is fixed, no trim coils on the hills will be needed, and the main coil can be a single electrical circuit which simplifies cyclotron operation.

A sensitive aspect of the design which has not been fully resolved at this time is the need to provide adequate space in the magnet for an electrostatic deflector to initiate the beam extraction process. The magnet used for the Figure XIII calculation had a 38.1mm aperture in the hill region which is quite tight relative to the details of a deflector which will desirably have a good field region of 10mm or more. Noting this sensitive situation, a second magnet calculation was performed with the hill aperture increased to 50.8mm. Figure XV shows the principal magnetic effect of this change, namely a reduction in the 4th harmonic content of the azimuthal

variation of the field. Orbits in each of these fields were tracked by numerically integrating the equations of motion for a selection of orbits at different energies; results of these calculations for the very important axial focusing frequency (plotted as "NU Z", the ratio to the orbital frequency) are given in figures XVI and XVII. The 38.1mm magnet gap gives a NU Z which is somewhat stronger than the 0.15 value usually taken as the design goal, whereas the 50.8mm field gives a NU Z which, in the vicinity of 175 MeV, is too low. The weak spot in the 50.8mm field can be in part filled in by allowing a local deviation from the isochronism condition which will be explored in future studies; a magnet gap in the 45 to 48mm range is a likely final result.

Assuming that an appropriate electrostatic deflector can be realized, Figure XVIII shows the calculated central ray of the extraction orbit, the first two boxes on the orbit indicating the position of electrostatic elements and the remaining boxes denoting magnetic elements (inert iron bars arranged to give dipole and quadrapole fields). In general the extraction orbit is well behaved; displaced trajectories experience focusing in both transverse coordinates and the beam exits the machine on a reasonable trajectory. An interest which is new relative to previous positive ion cyclotron experience is a desire to extract the beam on opposite sides of the cyclotron, preferably without needing to move mechanical elements. The feasibility of such a process depends on whether the orbit at an angle 180° earlier was at a radius which would cause it to collide with any part of the second extraction system. After some manipulation, orbits satisfying this constraint were obtained; Figure XIX is a (rectangular) radius vs. azimuth plot showing the extraction central ray as a solid line, the outer envelope of all preceding rays as a dot-dash line, and the envelope function 180° earlier as a dotted line. The clearance between the extraction orbit and both of the envelope functions establishes the feasibility of the dual extraction concept. Selection of one extraction path or the other would be accomplished by flipping a small magnetic first harmonic of about 0.3 milliTesla which can happen quickly.

The studies described above clearly establish the general feasibility of the 3 Tesla, 220 MeV, isochronous cyclotron and allow it to be considered on an equal footing with other cyclotron concepts in considering the selection of an optimized accelerator configuration for a proton therapy system for Princess Margaret Hospital. Assuming the rf system will operate on a low duty factor pulsed basis (following the very successful recent experience with the Harper Hospital cyclotron), an isochronous cyclotron can clearly be a highly competitive system in the sense of efficiency and cost effectiveness.

IV. POSSIBLE ARCHITECTURAL LAYOUTS

The architectural arrangement which is already in place at Princess Margaret for new electron accelerator rooms fixes a building pattern which most easily matches with a straight line arrangement of accelerator and treatment rooms. A building arrangement in which the accelerator is surrounded, or partially surrounded by a fan of treatment rooms, as in Figure XX, is a distinct mismatch and arrangements of this type have therefore been omitted from consideration. The objective of this section is then mainly to present a sequence of possible therapy facility layouts superimposed on the architectural grid of the new hospital. The set of drawings includes several different assumptions as to the accelerator system, the gantry structure, the

strength of the gantry magnets, the thickness of the shielding, and the access system to the high radiation areas.

The building layout figures include a variety of shielding configurations some of which assume earth as an adjacent material on the west and some of which do not. The sequence also includes different types of entry doors and mazes. All of these features are major factors in adapting a given accelerator and therapy room system to the Princess Margaret Hospital plan. At this point in time, the key shielding parameters, thickness and material, are difficult to precisely specify, since the required shielding mass under PMH radiation regulations will depend on the duty factor with which the accelerator will be used, the fraction of treatments which use full beam, the occupancy factor of the space outside the shield wall, the nature of the population in the area to be protected, etc.

Three shield thicknesses which occur frequently in the sequence of floor plans are 155cm, 185cm, and 215 cm. To provide a qualitative feeling for the effect of such walls, levels of radiation transmitted through such shields in a typical situation are given in Table I. The radiation level at the shield exit point depends on the distance of the stopping target from the shield, the direction of the beam relative to the point at which the radiation level is being calculated, the number of protons per second incident on the target, and (weakly) on the material of the stopping target. The variety of options is too broad to review in a thorough way, but a set of values for a few typical conditions is given in Table I and from these the approximate radiation levels at other points can be inferred. The calculations in the Table are based on a set of measurements made at Fermi Lab by DeLucca and Siebers [16] using beams from the Loma Linda accelerator. The beam stopping point is taken to be 3m from the shield, the stopping current is assumed to be 16.7x10**12 protons per minute (one of the highest values from a Table by Goitein [17]), and entries are given in rem/hour for three shield thicknesses (155, 185, and 215cm of normal 2.3 gm/cc concrete) and at four angles relative to the beam direction. If a beam of the assumed intensity is used full time on the thinnest shield, the resulting radiation levels would not be acceptable. With the thicker shields and with allowance for a relatively low beam on time, the results are marginally acceptable. The 0° direction relative to the beam is of course the most difficult problem -- a 50cm iron beamstop can fairly easily be incorporated in a gantry structure (and trivially in a fixed beam facility) -- such a thickness reduces radiation levels by an added factor of ten. Alternatively, a high density concrete could be used in some parts of the shielding wall. With one or another of these strategies radiation levels can be brought to needed levels with shields of thickness as shown in the various plans.

The layouts show three types of access protection namely a maze, which is the most convenient but least compact, and vertical and horizontally moving doors. Doors which move vertically are the most compact (on the main floor level) but require a pit below the door and a hydraulic system as a utility. Any of these access protection options could be adapted to each of the plans depicted in Figures XXI through XXVIII -- judgments of architectural and operating convenience will need to guide the final selection -- the use of one or another design in a particular Figure is largely arbitrary and primarily intended to display principal features of each system.

Figures XXI and XXII are vertical and plan views of the most compact system, namely, a therapy facility in which the accelerator is a 5T

Table I. Radiation levels at the exit surface of ordinary concrete (2.3 gm/cc) shields of three thicknesses and at four angles relative to the primary beam. Assumed proton intensity is 16.7*10**12 protons per minute on a stopping target located 300cm from the entry surface of the shield. Attenuation lengths and source strengths are taken from the 230 MeV study of DeLucca and Siebers [16].

Shielding Measurements from ref. 16				Dose at outside of shield (300 cm + shield thickness)= distance from source		
Angle relative to proton beam	Attenuation Length in $\rho=1.88\frac{gm}{cm^3}$ concrete	Attenuation Length in $\rho=2.3\frac{gm}{cm^3}$ concrete	Production strength $\frac{rem.cm^2}{proton}x10^{-10}$	Shield thickness 2.3 gm/cm^3 concrete 155 cm	185cm	215cm
0°	47.1 cm	38.0 cm	63	0.52 rem/hr	0.21 rem/hr	0.083 rem/hr
22°	45.4 cm	36.6 cm	33	0.23 "	0.090 "	0.035 "
45°	41.3 cm	33.3 cm	13.4	0.062 "	0.022 "	0.008 "
90°	30.8 cm	24.9 cm	4.1	0.004 "	0.0010 "	0.0003 "

superconducting synchrocyclotron and the gantry uses 3.5T magnets with beam spreading accomplished by using a line image system such as shown in Figure VIII plus motion of the patient.

Figures XXIII and XXIV show an arrangement intended to represent the largest combination of two treatment rooms and an accelerator room which could be fitted into the space which the architectural plans presently allot to one electron linac plus a Cobalt unit. The accelerator in this configuration is a 3T superconducting isochronous cyclotron and the gantry magnets assume 2.25T fields which gives a 1.0m bending radius, this bending radius being at the extreme limit of what might be attempted with room temperature coils, but much more probably in the superconducting coil regime. The spacing between the last bending magnet and the isocenter is 2.15m, or 2/3 of the value used at Loma Linda. This spacing should allow use of scatterers to spread the beam in the fashion of the presently used systems, particularly if a maximum field size of 15 cm is acceptable (as has been preliminarily stipulated at PMH). The drawings assume a floor level in the treatment room which is depressed by 1m relative to the normal building floor level; this feature showing clearly in Section A of Figure XXIII. Steps are provided for mobile personnel and a vertical hydraulic shield door could serve as an elevator for others and for equipment. The floor offset can be eliminated by raising the complete accelerator and treatment room complex -- a verbal discussion of this possibility at PMH in Dec. 1990 tentatively concluded that such a shift was compatible with other architectural requirements.

The facility arrangements presented in Figures XXI thru XXIV assume a rotating cyclotron. As discussed at an earlier point in this report, rotating the

accelerator so that the beam remains always in one plane makes construction more difficult but simplifies operation. Figure XXV in contrast shows a fixed accelerator system and corkscrew gantries laid out as 3 to 2 reductions of the Loma Linda gantries. The cyclotron is a 3T superconducting isochronous system but a room temperature 2T design would also fit in the space shown. The assumed gantry scaling implies smaller fields or thicker scatterers (as discussed in section I.A) than at Loma Linda and also stronger magnets, near the limit of room temperature technology. It would certainly also be possible to tradeoff magnetic field strength against treatment field size, i.e. superconducting magnets could give more magnet to isocenter spacing and therefore larger scattered fields, whereas less extreme room temperature magnets would give smaller fields. (As noted previously, at the Dec. 1990 meeting in Toronto, maximum treatment fields of 15 cm were tentatively stipulated as adequate for the anticipated therapy program at PMH.)

Figures XXVI and XXVII present a more radical facility arrangement namely one in which gantries are eliminated in the fashion of the new Japanese heavy ion facility at Chiba [18]. The facility is more compact and clearly less costly than any of the other options and provides the vertical and horizontal beams which account for the vast preponderance of present radiation therapy treatments and also beams at the intervening 45° angles. The complete system is greatly simplified with no major equipment needing to move. Beams are directed to the selected treatment line by simply turning the appropriate magnets on or leaving them off. (Presuming that this should happen in 10 to 20 seconds, a room temperature magnet system is probably indicated -- the figures therefore use a 1.4 meter bending radius.) The few patients who need "off angle" treatments could be positioned at a partially rotated angle if they were encased in a Loma Linda style patient pod [19] or on a probably simpler tilted table with a thin restraining barrier on the lower edge (maximum tilt of 1 in 2.5 needed to make all angles accessible); if treatment planning studies were made in the same pod or tilted table, the location of organs should be normally stable.

Finally Figure XXVIII shows a full size Loma Linda synchrotron positioned between two 3 to 2 scaled Loma Linda gantries. If one treatment room is omitted, the system fits the linac plus Cobalt unit site assumed for the previous arrangements. With two treatment rooms, a somewhat longer space is needed, but the architectural problem is perhaps not overwhelming. The principal advantage of this system is that the accelerator is based on an already operating design and is commercially available [13].

All of the plans given in the Figures focus on the radiation areas and neglect space required for utilities which must of course be provided in an actual building. If accelerator and beam transport are superconducting, a room of 5m by 10m should handle power supplies, rf drive, safety interlocks, refrigerator cold box, liquid helium storage dewar, etc. If room temperature magnets are used this area would double to about $100m^2$. Having the utilities area close to the accelerator is advantageous but not essential. The exact shape of the needed area is also mostly unconstrained but the corridor effect in a very long narrow room would take more space. Noisy equipment (refrigerator compressor, pumps for low conductivity water, pumps for hydraulic shield doors, etc.) is usually housed separately in a building equipment room and needs about $20m^2$. Having this equipment within 50m of the accelerator is desirable but further away is workable and mainly requires bigger connecting pipes. If a superconducting system is used, a warm helium

15 atmosphere storage tank with capacity of about $30m^3$(~3m dia. by 5m long) is also needed and can be fairly far away -- if 100m away the connecting pipe would need to be about 30 mm ID.

VI. SUGGESTED WORK PLAN

Planning of a proton therapy facility for Princess Margaret Hospital is now at a stage where tentative decisions need to be taken relative to major facility characteristics in order to restrict the range of further technical explorations. Needed decisions concern the choice of accelerator and the layout of the treatment rooms. The treatment room issue is perhaps the most difficult decision and the decisions will almost certainly involve a large component of arbitrary or intuitive choice. Ideally, treatment plans would be developed for a set of typical disease conditions for a number of the promising beam delivery systems and these would then be compared, weighing the incremental increases in cost vs. incremental gain in treatment effectiveness, in order to arrive at an economically optimized design. The work involved in making such a comparison is obviously large -- probably too large to be a realistic expectation; joint efforts with other institutions can help and should clearly be explored. At least one full time treatment planner (backed up by frequent consultations with medical staff) would desirably be assigned to such an effort for a year or more to make a significant impact. If such an effort can be mounted, there will be an important added benefit in providing a broader knowledge base to use in the future in guiding the many detailed implementation decisions which will come up as construction of the facility proceeds, helping at each point to guide mid-project decisions in directions which will optimize longterm medical effectiveness of the facility.

A first central decision should compare the fixed beam therapy room option vs. the several gantry systems. The fixed beam option will reduce the cost of the overall facility by about 30% in comparison with the gantry systems and the beam distribution system will be easier to operate. It is also the most compact system. In the rare circumstance of treatment plans involving use of angles other than the even 45° locations, a special cushion slanted by up to 22.5° (slope 10cm vertical per 25cm horizontal) would be needed. Consideration of such a configuration would then want to consider what fraction of the patient load would be expected to need non-standard angles and how much added time would be required to position this special group of patients. The magnitude of savings at issue in this decision would also easily justify visits to Chiba and Loma Linda by senior hospital staff in order to personally hear and evaluate the facts which led to selection of the fixed beam and gantry options respectively at these facilities.

If a fixed beam configuration is adopted the issue of beam spreading is less critical since the layouts provide adequate room for the contemplated beam spreading systems. If a gantry is selected, the opposite is the case -- beam spreading is a multi-million dollar issue -- if a gantry is to provide space for scattering of the beam after the last magnet, its size will be much the same as the Loma Linda gantries. The various proposals for spreading the beam prior to the last magnet (which markedly reduce the gantry size) all need considerable further accelerator physics analysis to study ion optical characteristics of the magnet systems and to check with Monte Carlo calculations the field flatness which will actually result, how this flatness will change as larger or smaller fields are used, and, if a variable energy

input beam is used, what are the parameters and flatness results at different energies. This is a considerable effort and desirably a "most likely" system would be tentatively picked in advance so that most of the study effort could concentrate on one system.

The conservative gantry decision is to provide space for scattering after the last magnet, this being the one system which is at present known experimentally to work well in medical use. The gantry size required for a scattering system can be somewhat reduced by agreeing to use smaller fields; the decision tentatively made in this direction at the meeting in Toronto in Dec. 1990 should be backed up by specific treatment planning documentation preferably including visits to centers such as Loma Linda, Berkeley, and MGH, where large fields have been judged to be medically important. If a small field design is selected, a report putting the basis of the decision on record would seem important, since such a decision will obviously be subjected to significant future criticism if some large group of patients is thereby excluded from treatment -- in this circumstance it would be important to have documentation evidencing that the decision was not made casually.

For the several gantry options, the penetration depth vs. field size tradeoffs involved in optimized scattering systems (such as those shown in Figure V) need to be weighed against anticipated medical needs. (Short flight paths reduce penetration due to added energy loss in the scatterer and also give more conical treatment fields with associated higher skin dose.) Desirably a medical physics study by PMH staff, or through collaborations with other institutions, would evaluate these issues and show their impact on a selection of typical treatment plans.

The medical benefit of energy variability is another issue which needs to be carefully weighed. The least expensive way of adjusting the penetration depth to match the need of a particular treatment situation is to set the depth entirely with loss of energy in matter such as for example by providing a bolus whose thickness added to the needed penetration depth corresponds to the range of a 220 MeV particle. With this system the sharpness in depth of the distal edge of the treatment field will be the same at every depth, which then gives up the possibility of sharpening the distal edge for shallow treatments by using an entering beam of lower energy.

The differences in the distal edge of a 250 MeV and a 100 MeV beam stopping in water is shown quantitatively in Figures XXIX and XXX. These results are calculated with a Monte Carlo code [20] which is believed to include all significant phenomena. The upper plot in each Figure gives the distribution in range of a group of 1000 monoenergetic ions incident in the direction of the x axis at y=z=0, the ions in Figure XXIX having 250 MeV energy and those in Figure XXX 100 MeV. The tabular material at the left of the plots shows a longitudinal straggling of 3.7 and 0.82mm respectively, (this quantity being the "sigma" of a gaussian distribution fitted to the range data). If the distal edge is assumed to start at the point where the dose drops to 95% of the peak value, it will drop to 42% of the peak value in a further step of one sigma (3.7 or 0.82mm respectively for the two energies) and to 7% of the peak value in a second one sigma step. Adequate protection of sensitive downstream tissue will be achieved somewhere between these two levels, but closer to the one sigma point than to the two.

A move of 1.25 sigma from the 95% point gives a dose of 29% of maximum, a likely working point. At 220 MeV the sigma length for the range straggling is

3.0mm and at 100 MeV it is 0.82mm; multiplying each of these by 1.25 and subtracting gives a sharpness advantage of 2.7mm if a 100 MeV incident beam is used for treatments at 7.5cm depth vs using the degraded 250 MeV beam. A judgement must then be made as to the incremental medical benefit of the 3mm sharper edge vs. the additional facility cost associated with providing variable energy beams.

(The preceding discussion is based on calculations which assume monochromatic incident beams since the Monte Carlo code does not provide incident beam energy spread as an option. Adding energy spread to the incident beam will further degrade the distal edge but the quantitative change will be small, since the beam energy spread will be small compared to the effective energy spread of the range straggling and the phenomena add in quadrature. The Monte Carlo calculations are time consuming and results which are effectively equivalent can be obtained by using a single particle Bragg curve and spreading it with the range straggling given by the Monte Carlo results as shown in Figure XXXI. A code is being written to use this approximation to include initial energy spread and also initial dimensional and directional spread. When this code is in use, the corrections to the distal edge sharpness caused by these spreads will be calculated.)

If variable energy beams are to be provided in the new PMH facility, they can be obtained by either using a variable energy accelerator or by degrading the beam at the beginning of the beam transport system and reforming a high quality beam at the end (using dispersive magnets and a monochromatizing wedge as shown schematically in Figure VIII). With respect to variable energy accelerators, both the isochronous cyclotron and the synchrotron are usually constructed as variable energy devices. The cyclotron would however cost 50 to 60% more if it is variable energy and energy changes would take 5 to 10 minutes. The synchrotron cost would be unchanged (although it is from the start a considerably more costly accelerator than the cyclotron) and its energy can change in a few seconds. (For the quick energy change capability to be useful, the beam transport system must likewise change in a few seconds, which means that more expensive laminated magnets must be used.)

The second energy changing strategy mentioned above matches well with the cyclotron system. In this arrangement, the primary energy shift is made with a degrader just at the exit port of the cyclotron and after dispersing the beam, a secondary monochromatizing wedge is inserted at the midpoint of the transport system to correct the energy spread introduced by the primary degrader. Increased aperture needs to be provided in the transport system in this case and some beam will be lost but the sharpness of the distal edge can match that obtained from a variable energy accelerator to within measurement tolerances.

The selection of the accelerator system or systems to adopt for further exploration is another major area where a semi-intuitive choice needs to be made at an early point (in order to restrict the scope of the ongoing studies so as to reduce design costs and to speed the overall project). Possible accelerators have been reviewed in earlier sections of this report. The principal differences in the several approaches are in size and cost, all of the systems considered being clearly capable of providing adequate intensity (presuming the intensity limit in synchrotron systems will be brought up to a slightly higher level in any newly built synchrotron). Generally the synchrotron is larger than the cyclotron, but not so large as to be a complete mismatch with the Princess Margaret architectural layouts. It has easier

energy variation and if the cyclotron is to provide variable energy, it largely loses its cost advantage vs. the synchrotron. Superconductivity further decreases the size of cyclotrons and increases the cost advantage, but superconducting equipment requires a significantly more sophisticated level of accelerator staff expertise in order to keep such units operating reliably. A 3 Tesla superconducting isochronous cyclotron appears to be an excellent match to the Princess Margaret requirements, but a 2 Tesla room temperature cyclotron and a Loma Linda type synchrotron each have advantages which PMH management will wish to consider (commercial fixed-price availability [13] & [21], and for the synchrotron, an operating prototype in existence).

References

1. A. Koehler and W. Preston, Radiology 104(1972)191.

2. A. Koehler, R. Schneider and J. Sisterson, Med.Phys. 4(1977)297.

3. B. Gottschalk, Proton Radiotherapy Nozzle with Combined Scatterer/Modulator, Harvard Cyclotron Laboratory Internal Report HCL 9/17/87.

4. B. Gottschalk, Proton Nozzle design Program NEU, Harvard Cyclotron Laboratory internal report HCL 3/23/90.

5. M. Goitein (priv.comm.).

6. H. Blattmann, Rad. & Envir. BioPhys. 16(1979)205
E. Pedroni, Rad. & Envir. BioPhys. 16(1979)211.

7. Y. Jongen, G. Lannoye, A New Concept of Compact Isocentric Gantry for Proton Therapy, Ion Beam Applications internal report YJ/amv/3/5/90.
(A similar gantry system was proposed by E. Pedronia of PSI at the Spring 1989, PTCOG meeting at FermiLab.)

8. A. Koehler, Preliminary Design for a Corkscrew Gantry, Report of the Facilities Working Group, L. Verhey ed. (1987) unpublished.
J. Sisterson, H. Enge, B. Gottschalk, A. Koehler, & L. Verhey, Design Considerations for a Proton Beam Gantry, poster Amer. Assoc. of Phys. Med. meeting, Lexington, KY (Aug. 1986) unpublished.

9. W. Chu, S. Curtis, J. Llacer, T. Renner and R. Sorensen, IEEE Trans. on Nucl. Sci. NS-32(1985)3321.

10. B. Sherrill, J. Bailey, E. Kashy, and C. Leakas, Nucl. Instr. & Meth. B40/41(1989)1004.

11. R. Prechter, Loma Linda University Medical Center Gantry Presentation, Science Applications International Corp. internal report May 12, 1987.

12. G. Lawrence (private comm.)

13. Science Applications International Corp., 227 Wall St., Princeton, N.J. 08540.

14. H. Blosser, J. Bailey, R. Burleigh, D. Johnson, E. Kashy, T. Kuo, F. Marti, J. Vincent, A. Zeller, E. Blosser, G. Blosser, R. Maughan, W. Powers, & J. Wagner, IEEE Trans. on Mag. 25(1989)1746.

15. P. Miller (private comm.).

16. J. Siebers, Shielding Measurements for a 230 MeV Proton Beam, PhD thesis (1990) Univ. of Wis. Madison.

17. M. Goitein, Proton Beam Intensity, Mass. Gen. Hosp. internal report 1/21/86 revised 3/19/86.

18. Y. Hirao et al, Proc. of the 2nd European Particle Accel. Conf. 1(1990)280.

19. D. Miller (private comm.).

20. J. Ziegler, TRIM - 91, IBM Yorktown NY internal report 1/3/91.

21. Ion Beam Applications, Chemin du Cyclotron 2, 1348 Louvain-la-Neuve, BELGIUM.

22. H. Enge (priv. comm.)

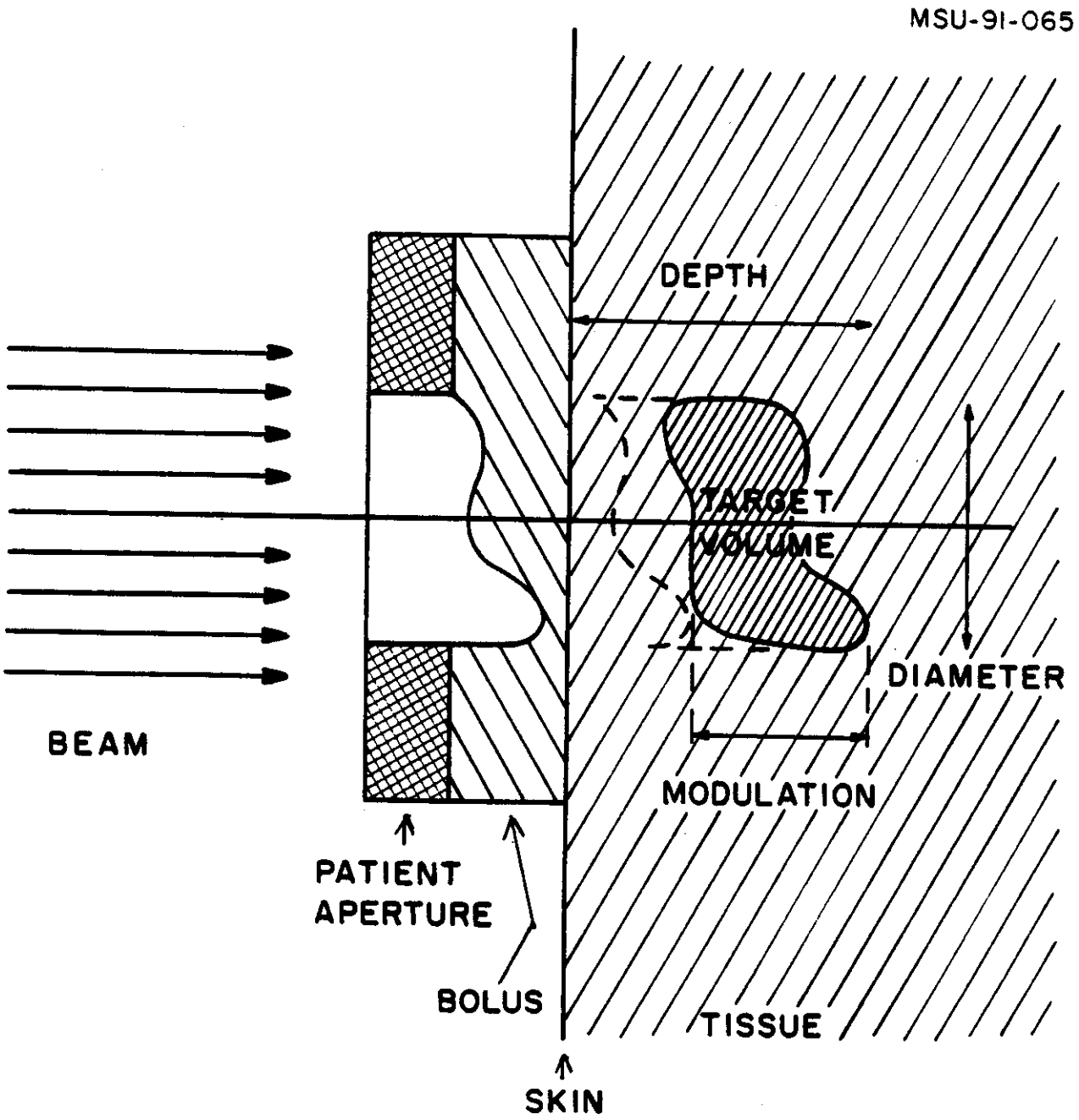

Fig. I. Schematic diagram showing use of patient aperture and bolus to shape transverse area and maximum penetration depth surface, respectively, of an assumed treatment volume. The bolus in this case is shaped to match the distal edge of the desired target volume as would be required if sensitive structures were located just beyond the target volume. (The total area treated with high dose will include the region inside the dashed line.)

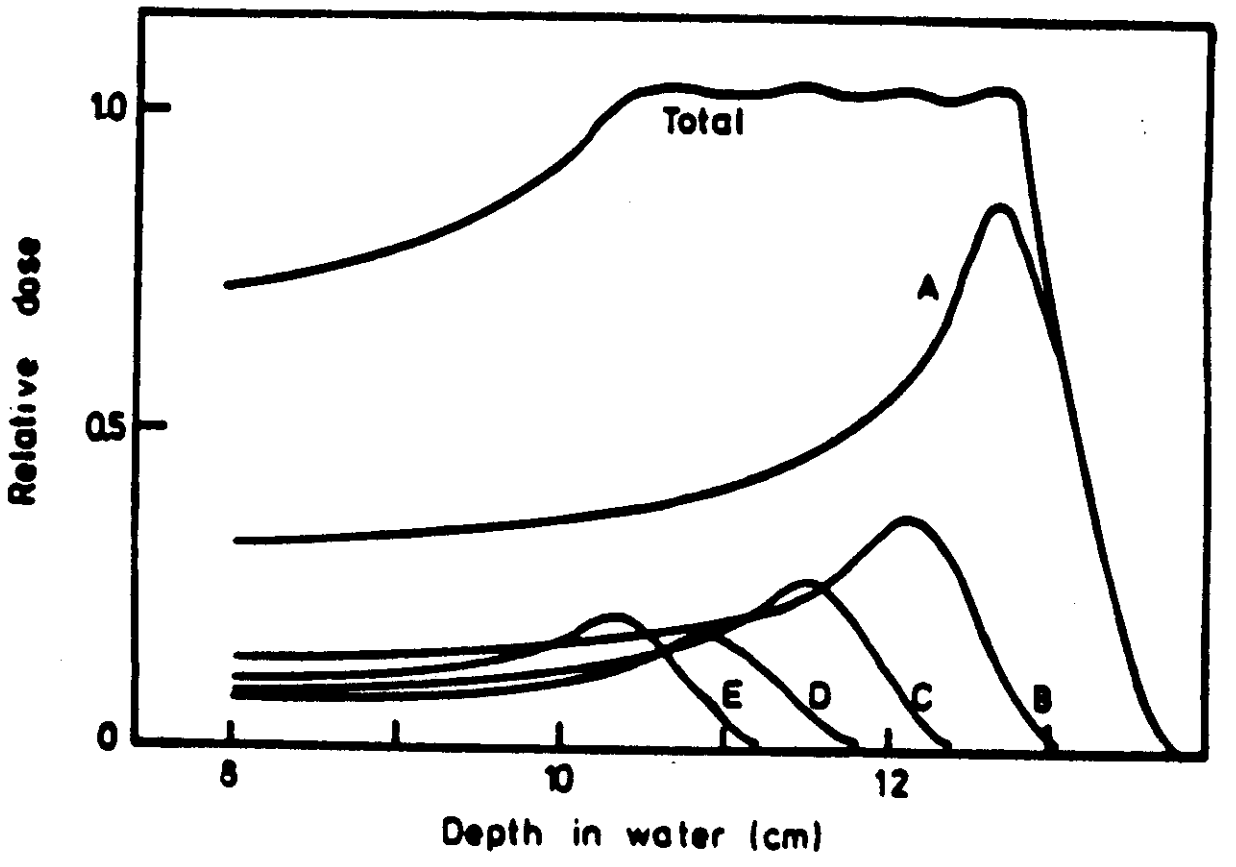

Fig. II. Schematic illustration of a combination of five individual Bragg curves for different energies, A, B, C, D, & E, with intensities adjusted to give a total flat dose region from approximately 10.5 to 13 centimeters, i.e., a "spread out" Bragg peak (from ref. [1]).

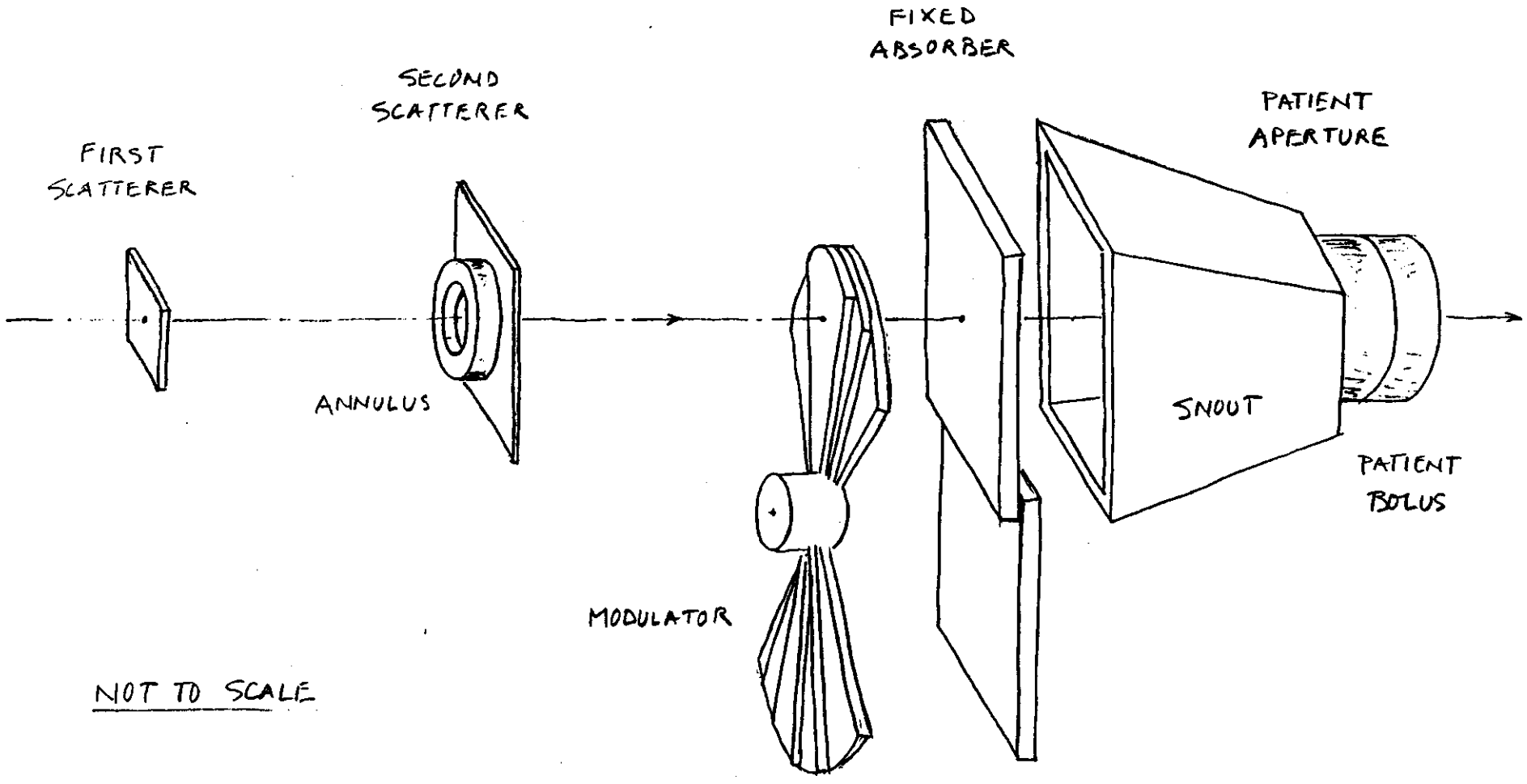

Fig. III. Schematic drawing showing the traditional arrangement of scatterers, modulators, aperture and bolus used for proton therapy at the Harvard Cyclotron Laboratory.

BG 3/6/91

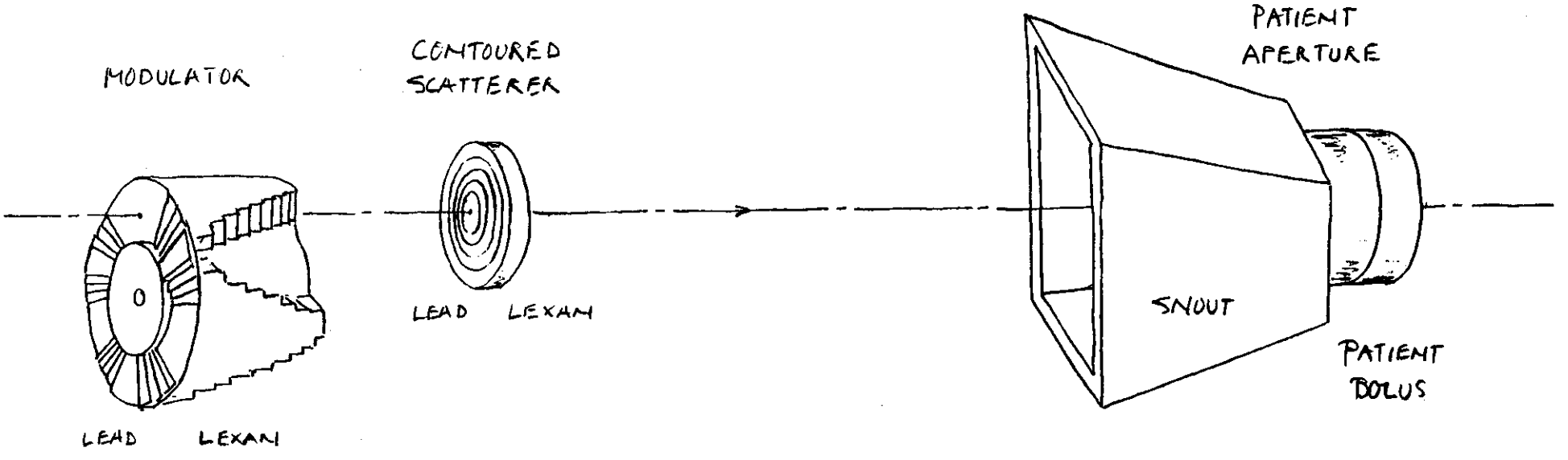

Fig. IV. Improved arrangement of beam line aperture proposed by Gottschalk (ref. [3]). Combined scatterer/modulator reduces penumbra at the patient and makes the beam line more compact.

BG 3/6/91

```
                    Copyright 1991 President and Fellows of Harvard College
                                NEU run   5-MAR-91  18:14:14

DESIGN.MOD                  .SCT, .MOD filename or DESIGN.SCT, .MOD
DESIGN.CON                  .ANN, .CON filename or DESIGN.ANN, .CON
MOLIERE                     MOLIERE, FASTMOL, HIGHLAND (Gaussian) or FASTHIGH
30NOV89T1211.BPK            Bragg peak spline file
- - - - - - - - - - - - - - - - - - - - - - - - - - - - - - - - - - - - - - -
                            1: pre scat or blank (material, upstr z (cm), g/cm2)
                            2: pre absorber or blank
LEAD          -1  -1        3: mod A mat'l (or blank for simple scatterer)
LEXAN          0  -1        4: mod B mat'l or 1st scat mat'l (Z4 meas = 15.9 cm)
                            5: post absorber or blank
LEXAN         -1 .061       6: 2nd scat A mat'l (or blank for annulus)
LEAD          50  -1        7: 2nd scat B mat'l
WATER        200  -1        8: WATER
WATER        206  19        9: WATER (tgt vol entrance Z, extent in depth)
- - - - - - - - - - - - - - - - - - - - - - - - - - - - - - - - - - - - - - -
220    0  8                  inc MeV, beam theta0 (mrad); desired flat radius (cm)
.95  .8  1                  dose tolerance level; Bragg level; cm/file unit
0  0  0                     depth linear, quad coeff; transverse quad coeff (%)
0  9 18                     up to 3 pullbacks (cm H2O) for trans scans, or 0's
.92  4  8  0                U0, # fitted radii, # output radii, max # passes
0 .5 1.1 1.75               starting radii (max 6/line)
.8155 .7137 .3119 .1068     starting proj scat strengths (max 6/line)
15 15 10000                 Q steps QA->QB, PHI steps 0->pi, lookup table size
15 5 11                     # steps, infty mult for norm int; # pts for FOM calc
.05 .5 .01 .001             init delta, red fact, give up test, convergence test
-5  30  -.1  1.1            z,y limits modulator picture (absolute Z)
-4  1  -6  6                ditto 2nd scatterer picture (relative to ZZ(7))
0  30  0   1.2              ditto depth dose (relative to ZZ(8) = tank entrance)
-20  20 0  1.2              x,y limits transverse scans
1 1 1 1                     playback factors for elts 3,4,6,7
1 30 1 0                    playback mod range, Bragg pks on/off, req'd norm const
- - - - - - - - - - - - - - - - - - - - - - - - - - - - - - - - - - - - - - -
Reference design, Princess Margaret 3T 220 MeV rot isochr, 2.15 m throw.

pass     avg     rms %    ys(1)    ys(2)    ys(3)    ys(4)    ys(5)    ys(6)
  0   0.09097  0.010   0.81550  0.71370  0.31190  0.10680

Used BPW.FOR on UM502.DAT with points added; FNAL raw beam at 232 MeV.
590   (?)  Z coord (cm) of scan Bragg peak
15   0.10000E+31   0.00000E+00  # pts, yp1, ypn
  3.0000   11.0000   19.0000   25.0000   29.4000   31.2600   31.7300  cm H2O
 32.3100   32.4000   32.6000   32.8000   33.0000   33.2000   33.4000
 33.6000
  0.3402    0.3447    0.3560    0.3943    0.5091    0.8005    0.9664  rel dose
  0.7461    0.5864    0.2690    0.1134    0.0225    0.0045    0.0011
  0.0016

   21    1.0000          # steps, cm/unit
  0.3516  0.1259  0.0955  0.0696  0.0576  0.0476  0.0402  0.0336   weights
  0.0295  0.0249  0.0220  0.0192  0.0171  0.0149  0.0128  0.0109
  0.0089  0.0068  0.0055  0.0041  0.0019
LEAD          first material
  0.3922  0.4251  0.4189  0.4119  0.4043  0.3960  0.3870  0.3772   thicknesses
  0.3667  0.3553  0.3430  0.3296  0.3151  0.2991  0.2817  0.2625
  0.2411  0.2173  0.1906  0.1600  0.1246
LEXAN         second material
  0.0000  0.6437  1.4829  2.3260  3.1728  4.0230  4.8768  5.7344   thicknesses
  6.5962  7.4625  8.3338  9.2103 10.0933 10.9833 11.8814 12.7888
 13.7074 14.6390 15.5860 16.5531 17.5456

    8   0.00000E+00   0.10000E+31    1.0000          # pts, yp1, ypn, cm/unit
  0.0000  0.4444  0.8889  1.3333  1.7778  2.2222  2.6667  3.1111   radii
LEXAN         first material
  0.0509  0.1742  0.6433  1.4096  2.0695  2.4256  2.5211  2.5211   thicknesses
LEAD          second material
  0.4949  0.4702  0.3763  0.2229  0.0906  0.0192  0.0000  0.0000   thicknesses

 -0.197  -0.202  -0.167  -0.107  -0.019   0.099   0.250   0.436     Z0(J) (cm)
  0.681   0.927   1.238   1.599   2.014   2.491   3.035   3.655
  4.364   5.172   6.097   7.163   8.400
   1.0115      0.91      798.2            skin/tgt dose, dose slope (%), norm const
      9.9       0.7        5.0            useful radius (cm), dose rms dev, pk-to-pk/average (%)
    46.23    100.43                       double integral to useful rad, single to infinity (%)
   24.060    24.685    25.000             lower 80, peak, upper 80 mod step 1 (cm H2O)
05MAR91T1814.MOD   05MAR91T1814.CON       files used and/or created
```

Fig. V-A. Input parameters and numerical results for the NEU [4] calculations for the reference design scattering system. The skin surface is 2.0m from the first scatterer and the target volume begins at 2.06m and ends at 2.25m, i.e. from 6 cm depth to 25cm depth.

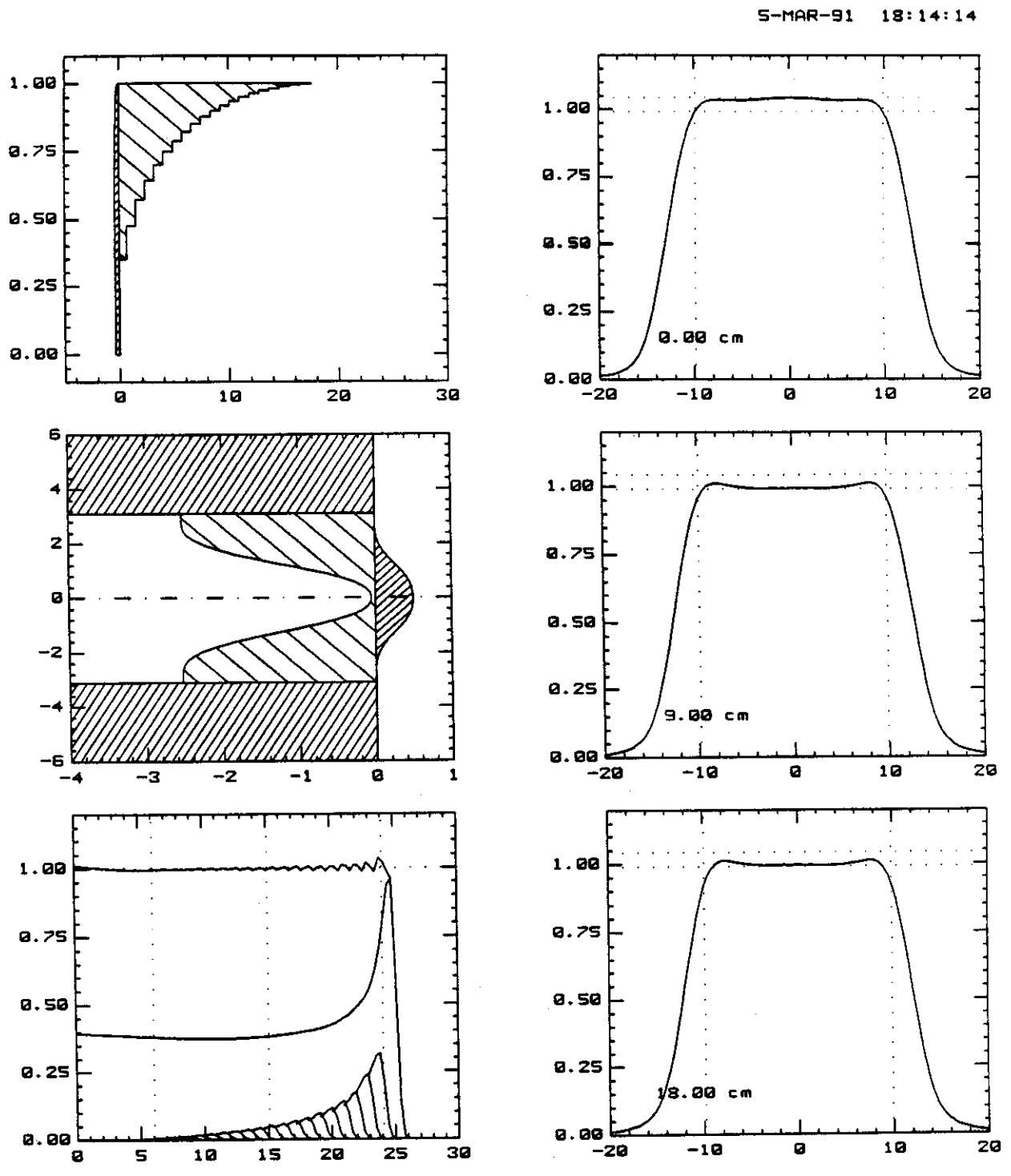

Fig. V-B. Graphical output from NEU. The horizontal scale on all graphs and the vertical scale on the left center graph are in centimeters. The vertical scale of the modulator/scatterer graph on the upper left gives the angular fraction of a modulator sector occupied by each element; vertical scales on other plots are dose in relative units. Depth labels on the three right hand plots are distance back from the maximum (i.e. 0.00 cm is 25 cm depth, 9.00 is 16cm depth, etc.)

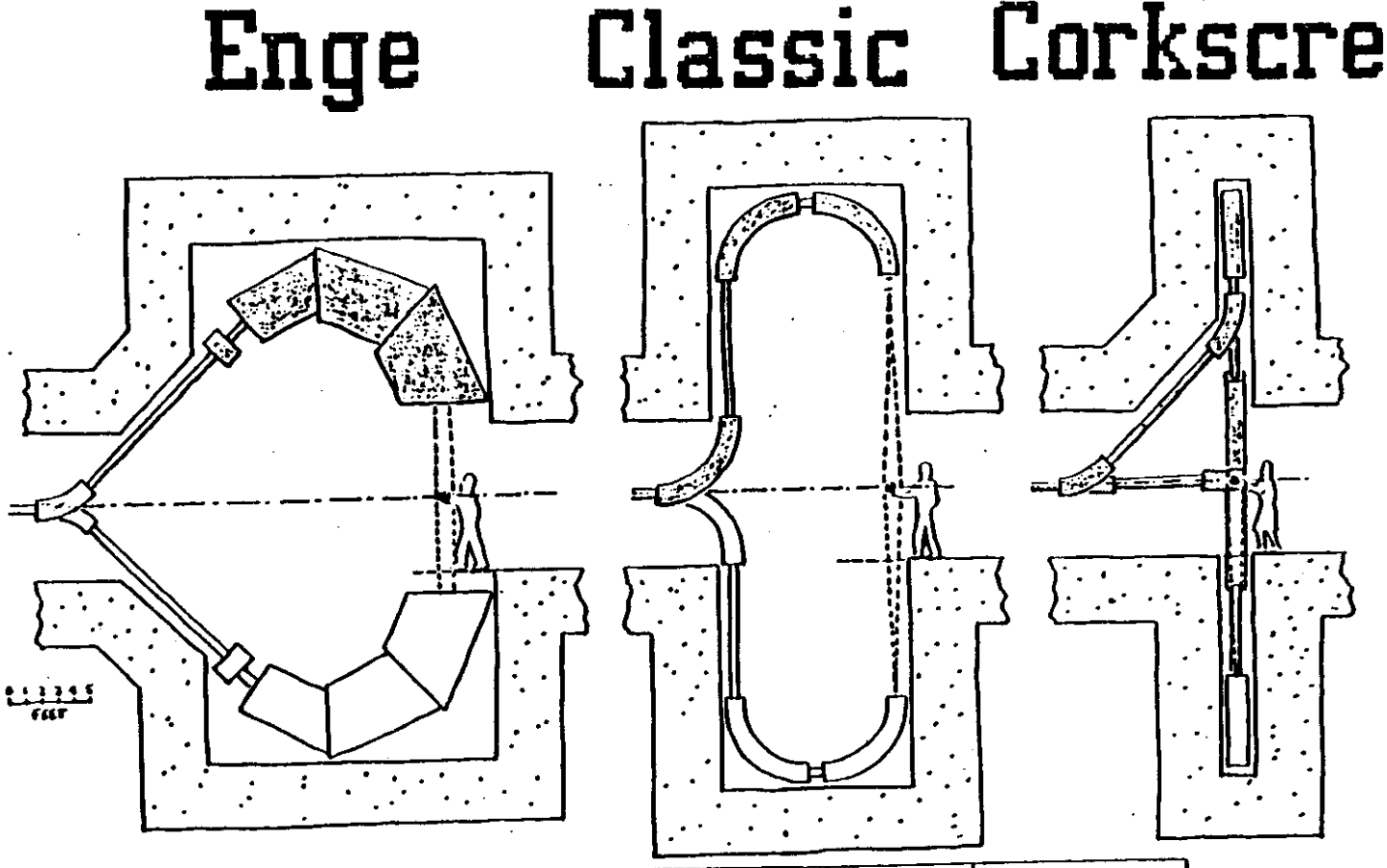

		ENGE	CLASSIC	CORKSCREW
gantry rotation	(degr.)	180 + 30	180+	180+
total bend	(degr.)	180	270	360
magnet power	(kW)	~ 170	~ 90	~ 120
magnet weight	(tons)	~ 40	~ 12	~ 18
total height	(ft)	39	45	45
gross bldg. vol.	(ft^3)	42,000	40,000	20,000
shielding	(ft^3 concrete)	23,000	24,000	18,000
	(tons concrete)	1800	1900	1400
design objective		reduce height and space requirement	simple design with known technology	save space and shielding
fringe benefits		∞ source distance rectangular field		easier floor design

Fig. VI. Schematic drawing showing design features of 3 important gantry arrangements (from ref. 8).

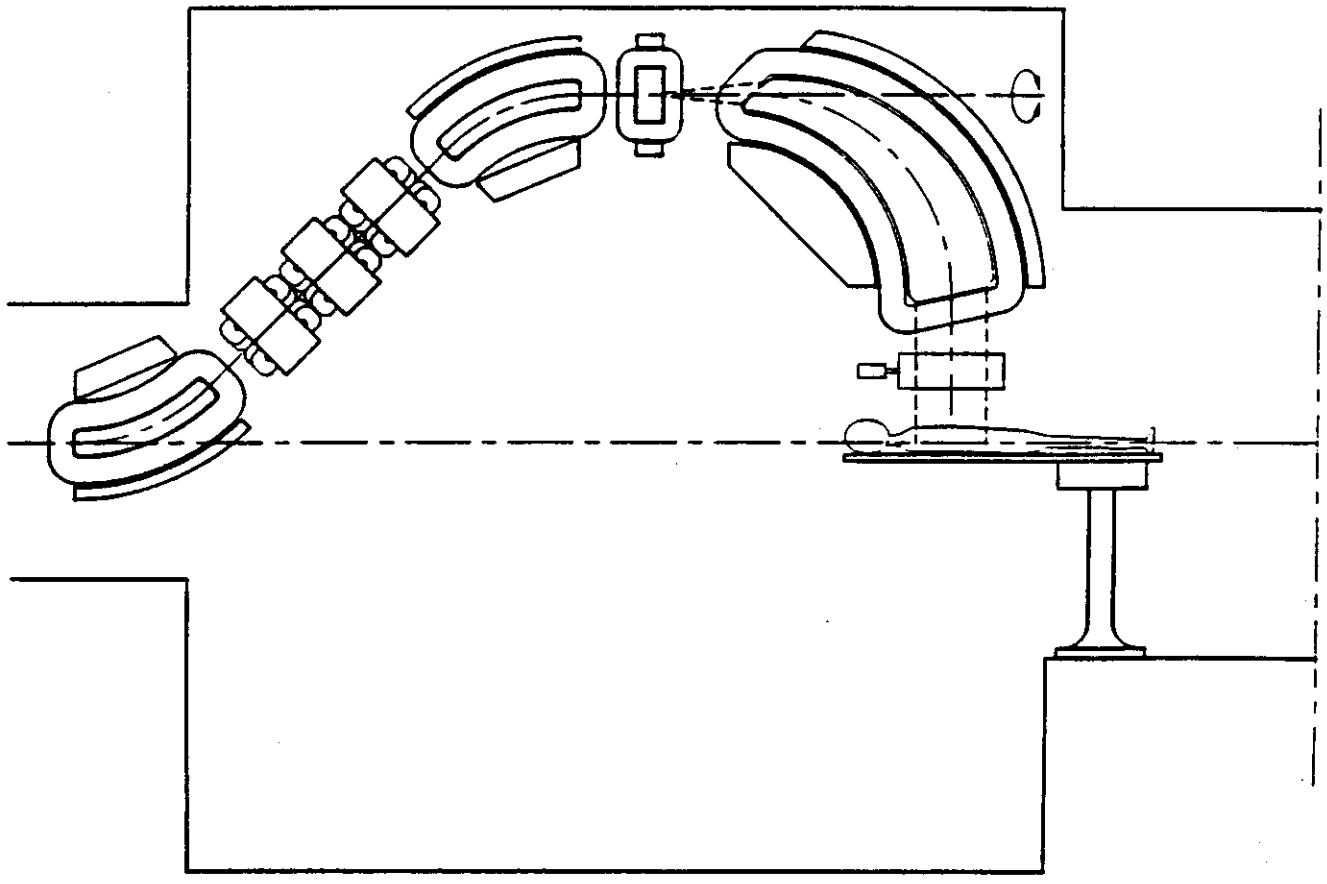

Fig. VII. Drawing showing gantry arrangement proposed by Jongen. The circular arrow at upper right indicates the rotation axis of the final magnet which sweeps the beam perpendicular to the plane of the drawing. The next-to-last magnet sweeps the beam in the plane of the Figure (from ref. 7).

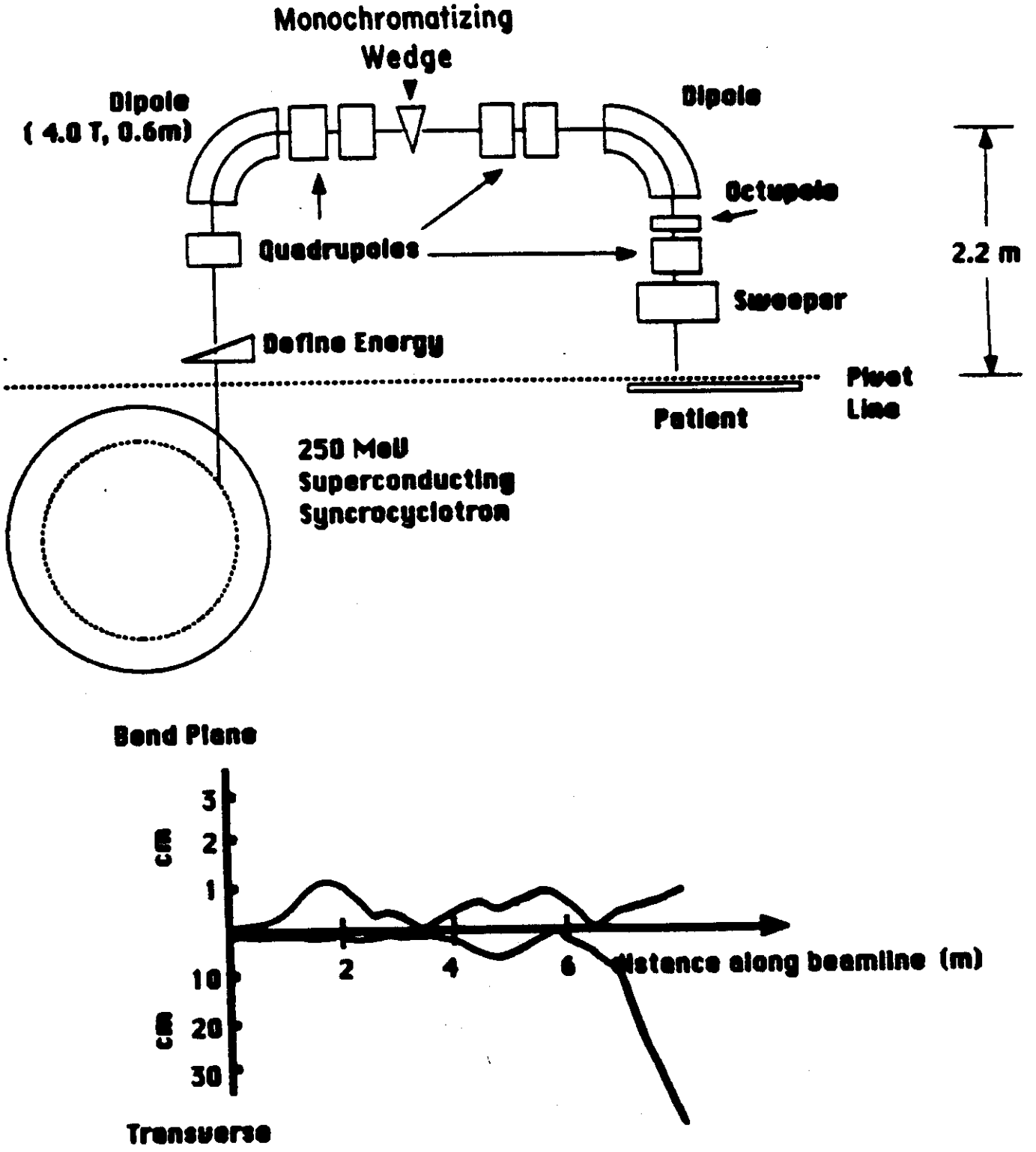

Fig. VIII. Drawing showing the gantry system proposed by Sherrill used in combination with a rotating accelerator and a graphite wedge to adjust the energy. The dashed line is the rotation axis of the system. The "Transport" output giving bend plane and axial envelopes of the beam is at the bottom.

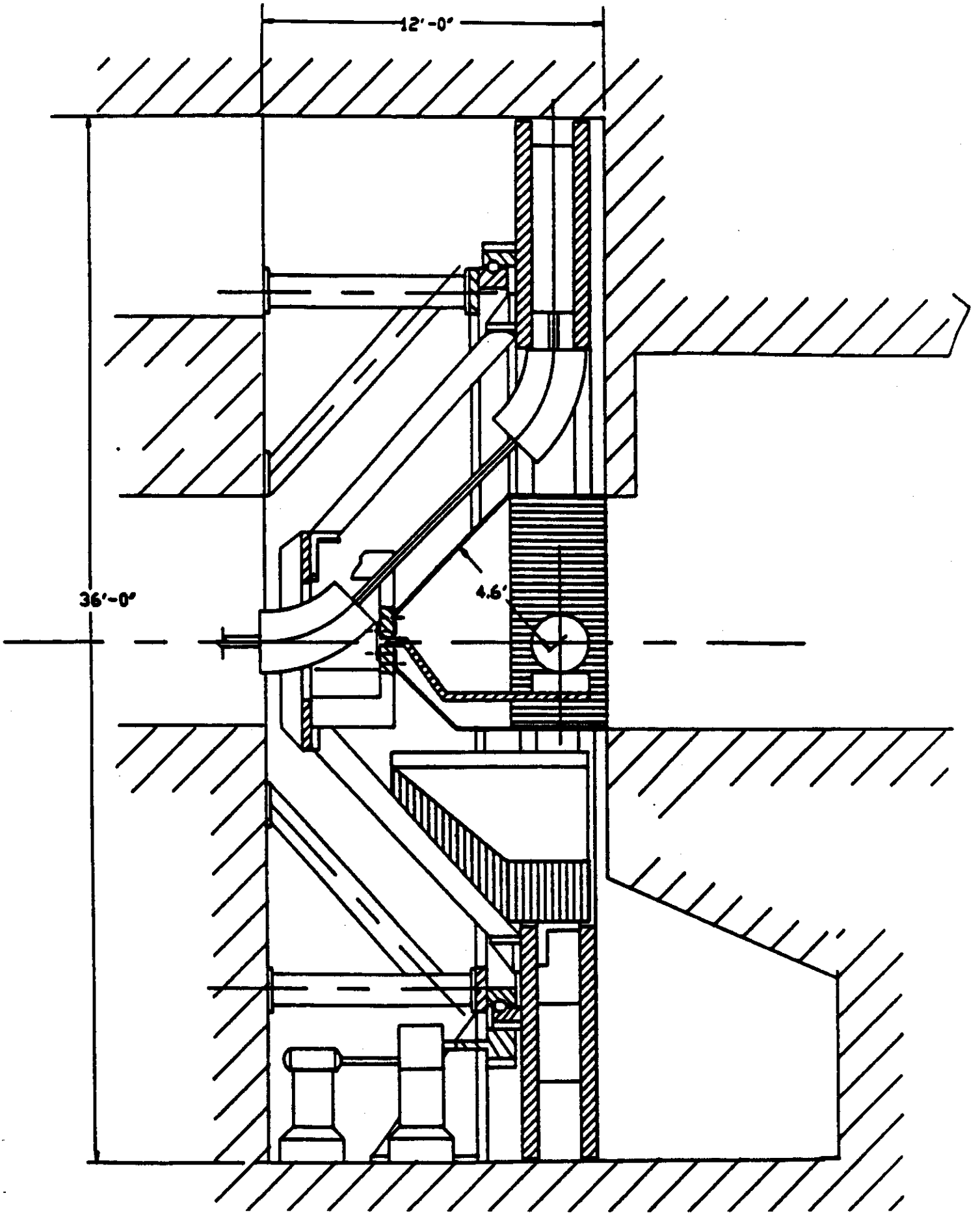

Fig. IX. Mechanical drawing of the Loma Linda gantry showing details of the support system. Note the 140 cm clearance (4.6') between the 45° section of the cork screw gantry beam line and the isocenter (from ref. [11]).

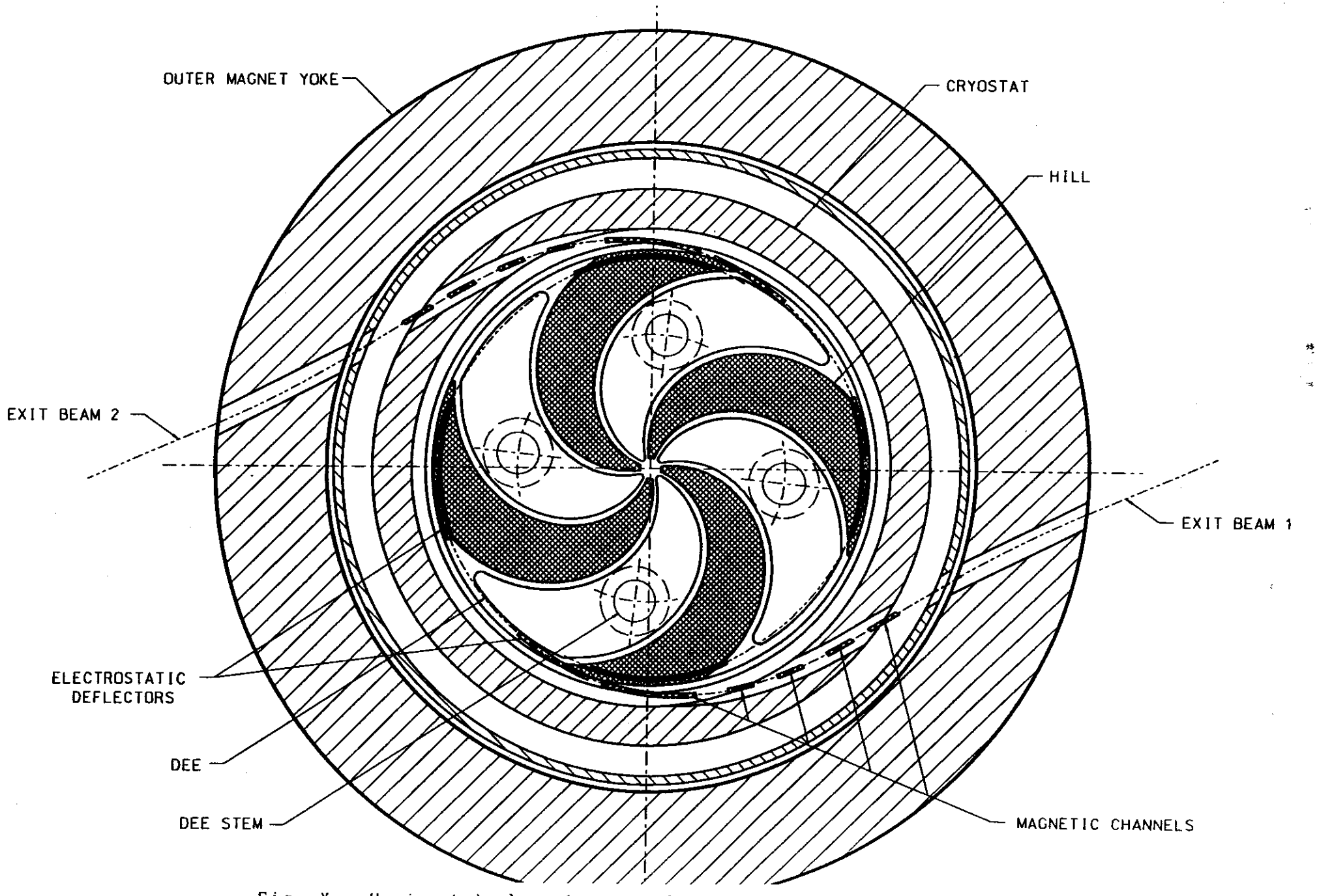

Fig. X. Horizontal plan view of a 3 Tesla isochrounous 220 MeV proton cyclotron. The hill and valley structure has a tighter spiral than is required (see text). A dual extraction system is shown conceptually.

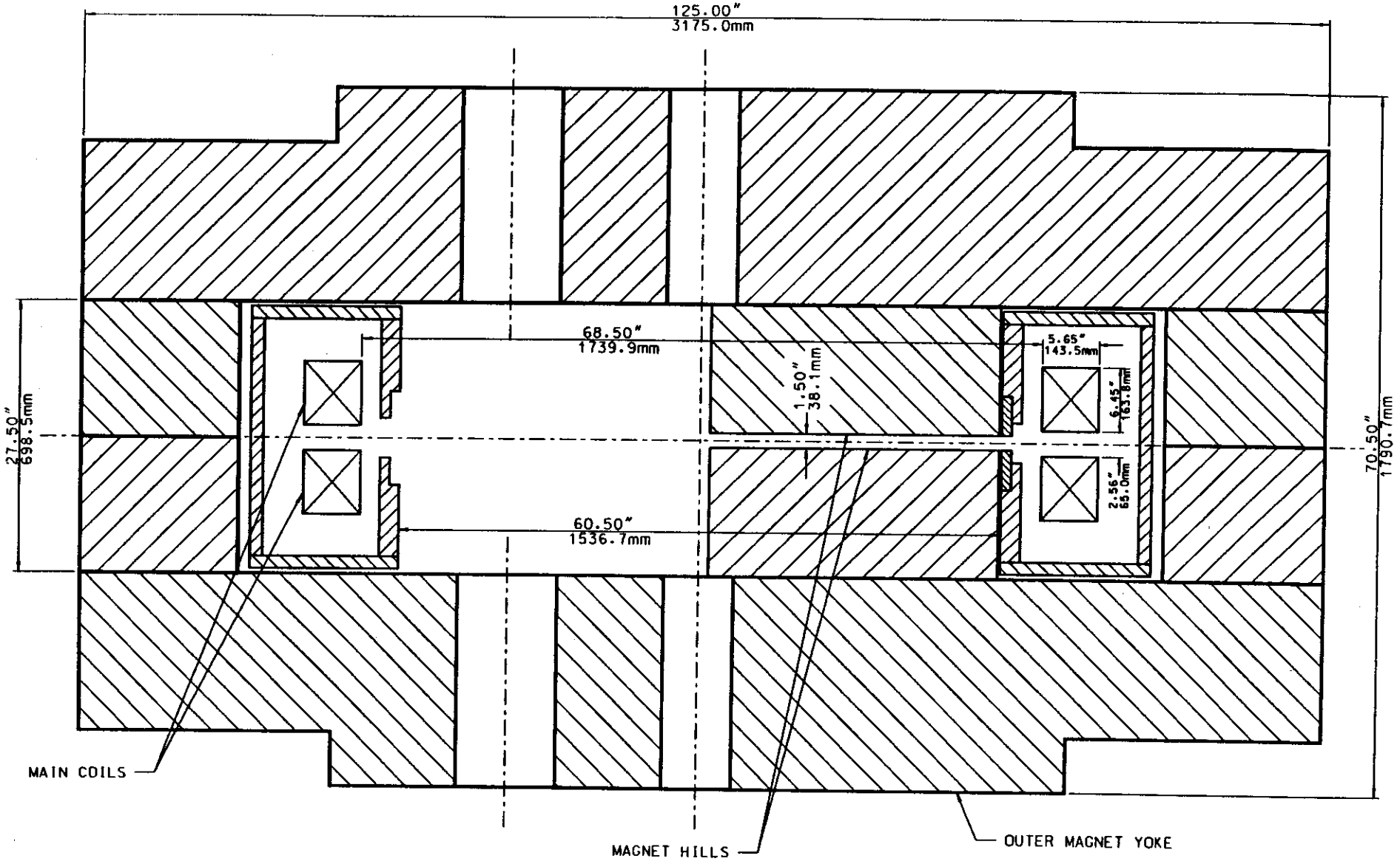

Fig. XI. Vertical section view of a 220 MeV isochronous proton cyclotron showing magnet hill on the right and magnet valley on the left. A nonmagnetic wall isolating the coil vacuum from the beam vacuum and a nonmagnetic helium vessel enclosure surrounding the main coils, are omitted.

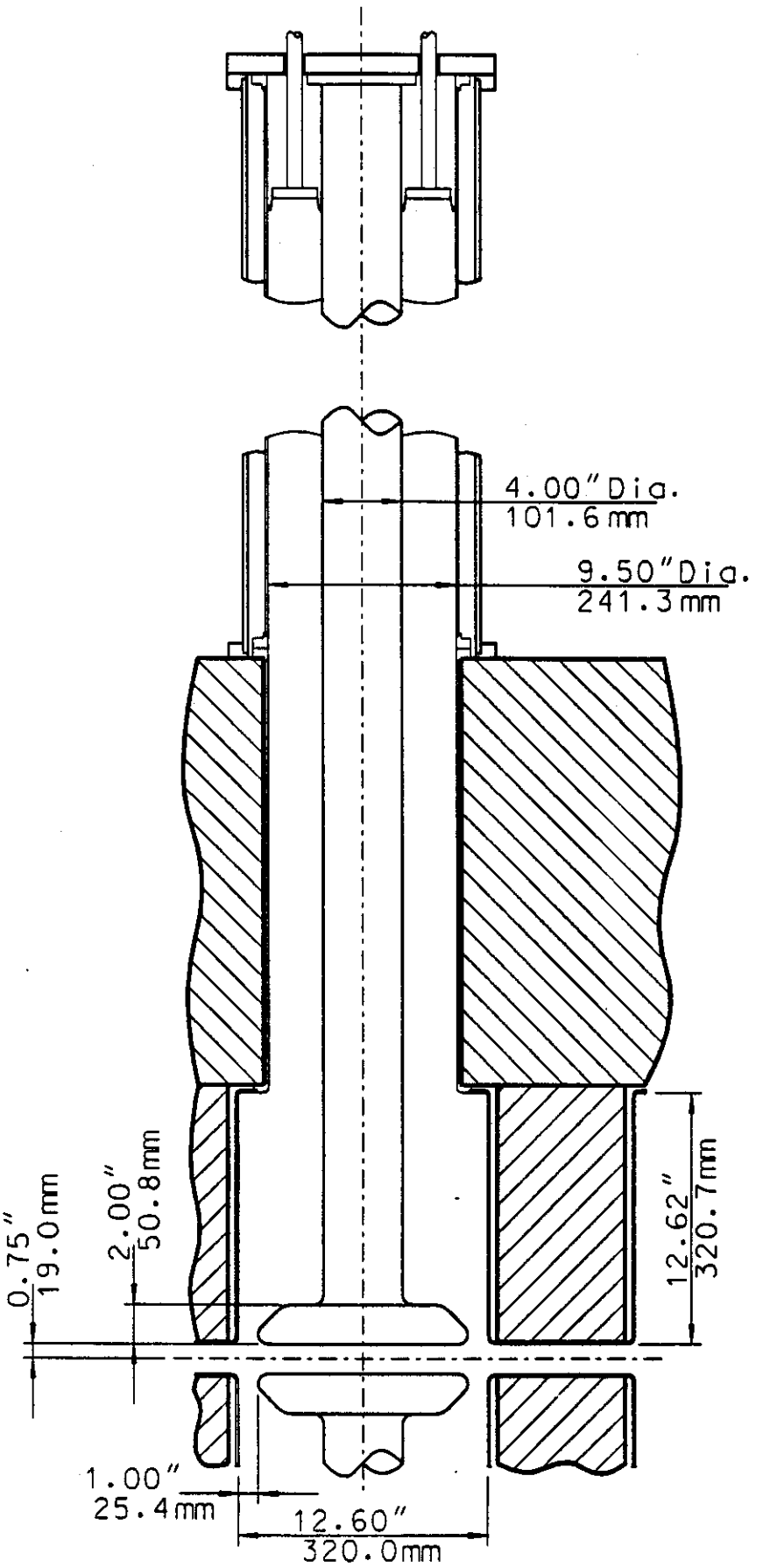

Fig. XII. Cross section view thru a dee stem of a possible 3 Tesla, 220 MeV isochronous cyclotron.

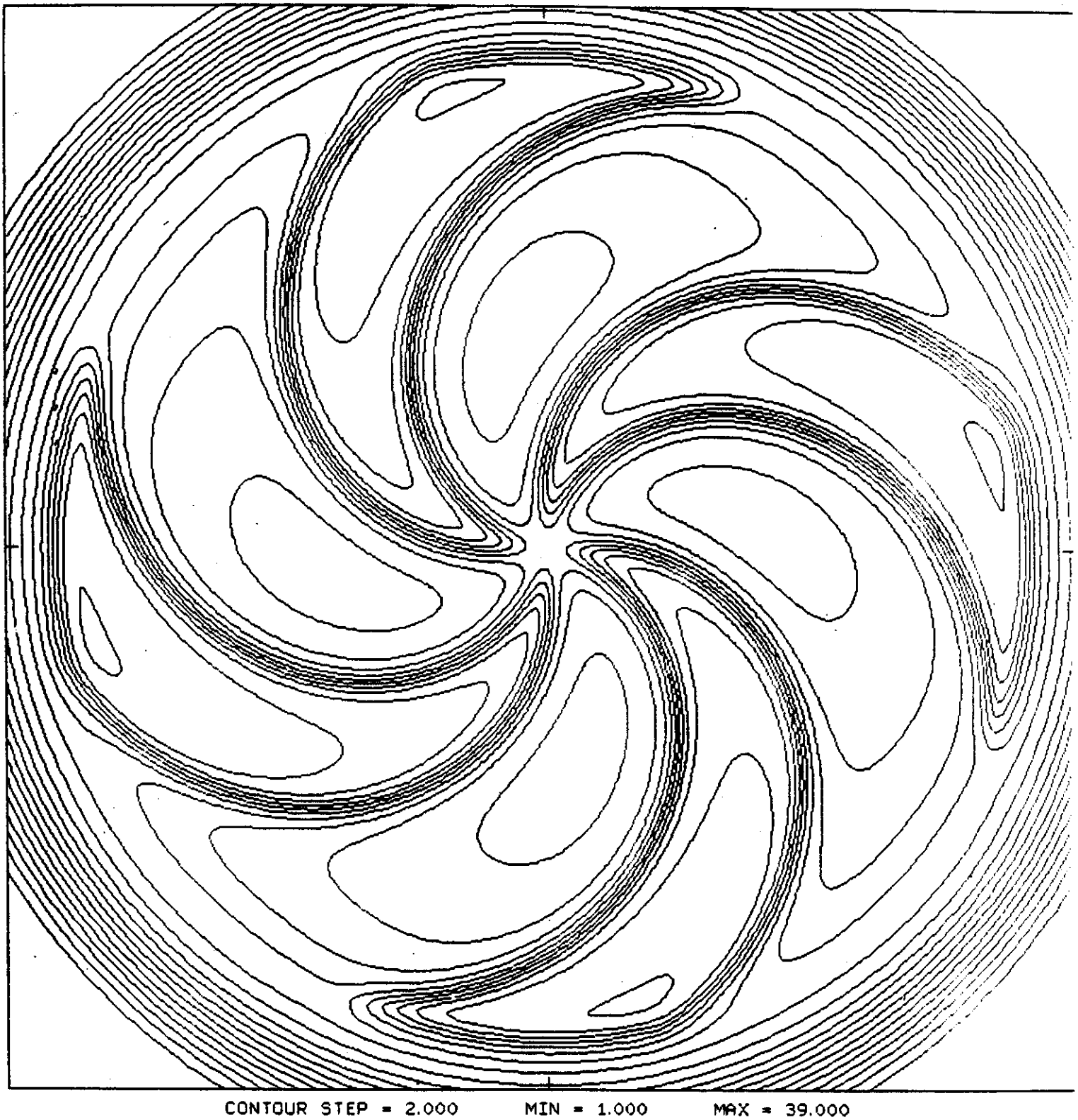

Fig. XIII. Calculated magnetic field for a 220 MeV isochronous cyclotron. The maximum contour line is 3.9 Tesla (the contour surrounding the small triangular region near the outer edge of the hills), the minimum contour is 0.1T (the interrupted large circle at the outside of the magnet), and the low contour in the bottom of the valleys at intermediate radii is 1.9 T.

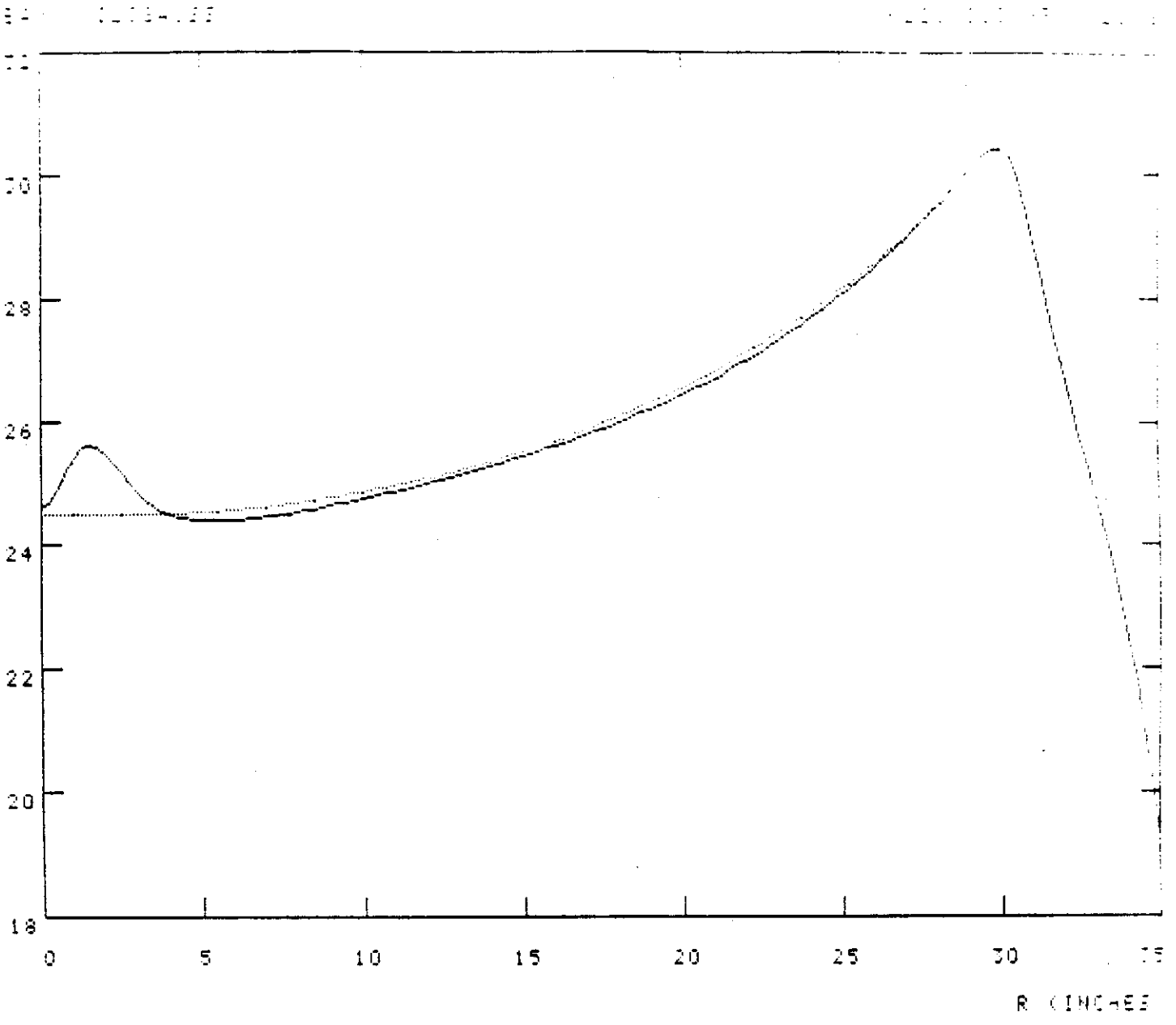

Fig. XIV. The azimuthal average of the magnetic field from Fig. XIII (solid line) versus the required isochronous average field (small dots). Further refinement of the iron shape will easily bring the two fields into accurate agreement establishing that a single main coil is adequate for such a cyclotron.

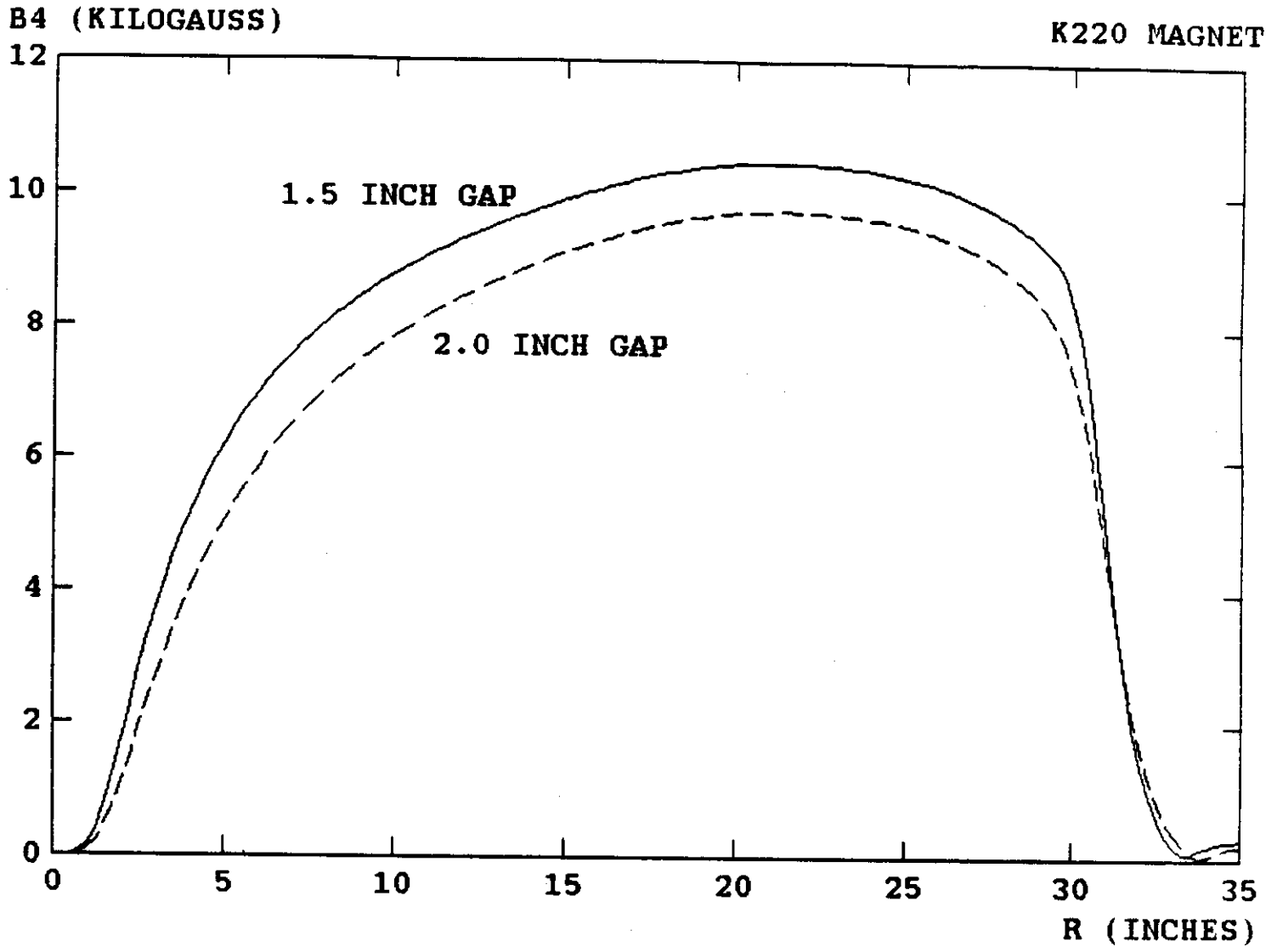

Fig. XV. The amplitude of the fourth harmonic Fourier component of the azimuthal variation of the magnetic field from Fig. XIII (solid curve), compared to the same coefficient for a magnet in which the hill gap is increased to 50.8 mm (the dashed curve).

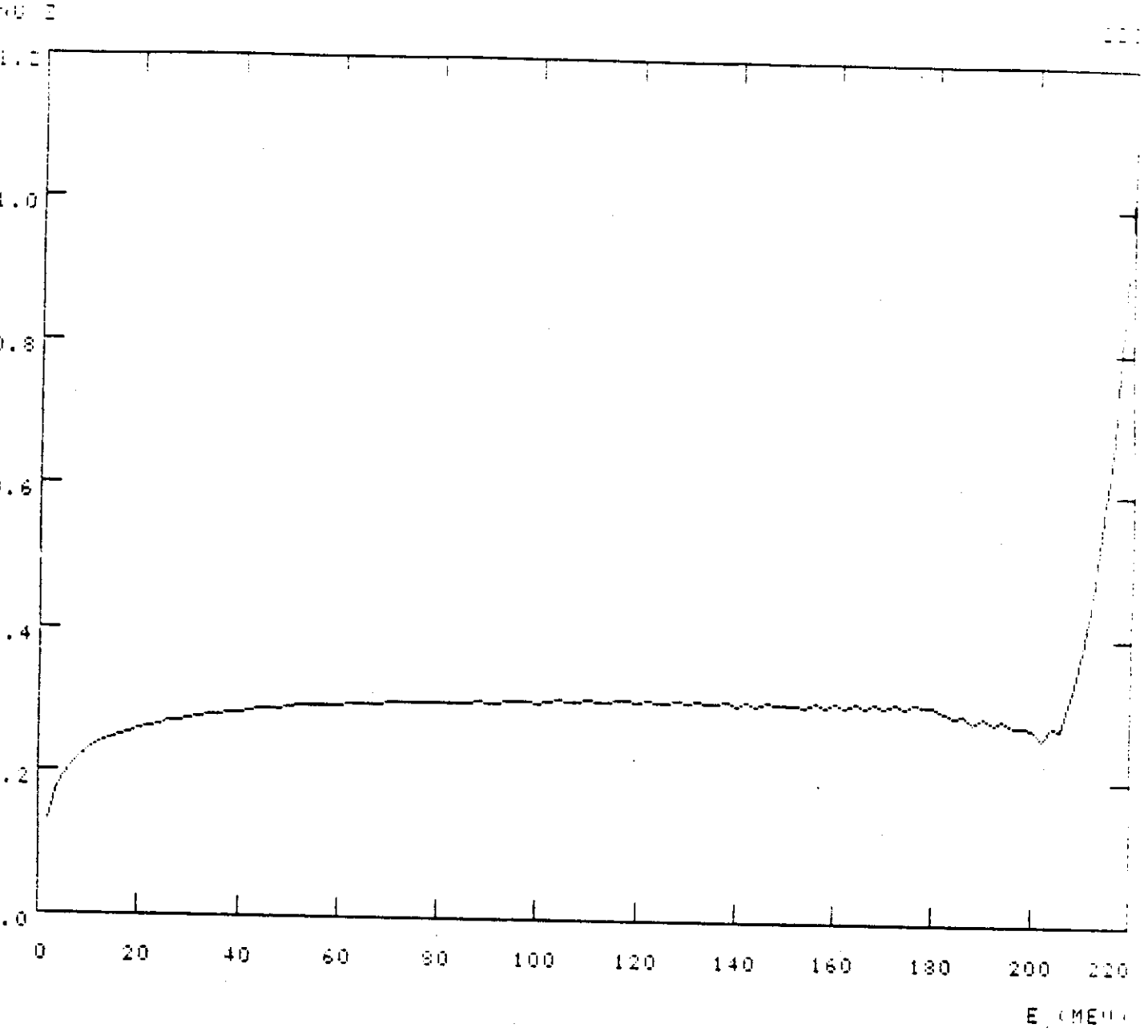

Fig. XVI. Axial focusing frequency versus energy for the magnetic field from Fig. XIII. A focusing frequency of 0.15 is usually considered adequate, i.e. the azimuthal variation of the field of Figure XIII is somewhat stronger than is really needed.

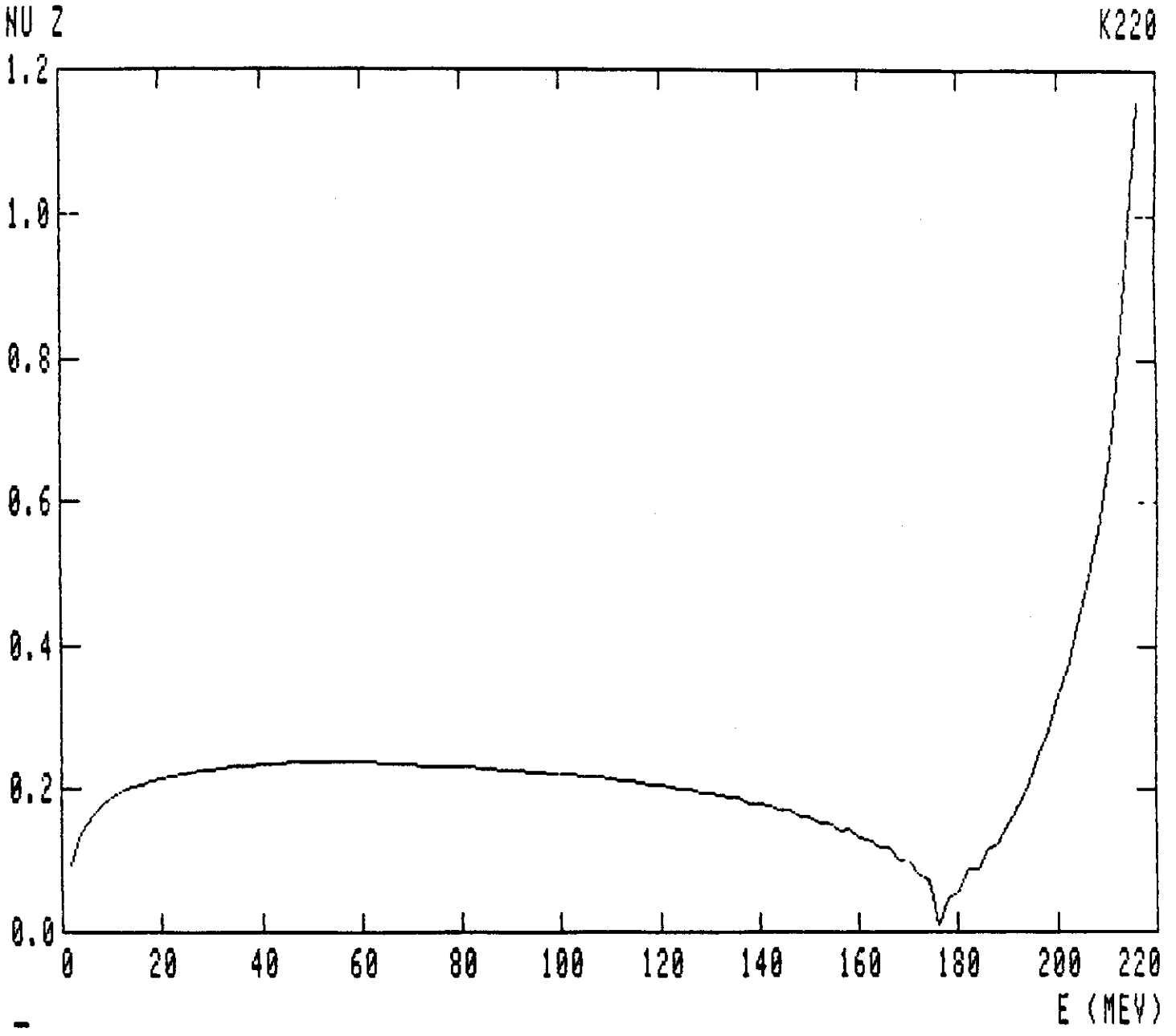

Fig. XVII. Axial focussing frequency versus energy for the field with magnet hill gap increased to 50.8 mm. The frequency is near 0 in the vicinity of 175 MeV, i.e. the increased gap is an over correction relative to the field of Fig. XVI.

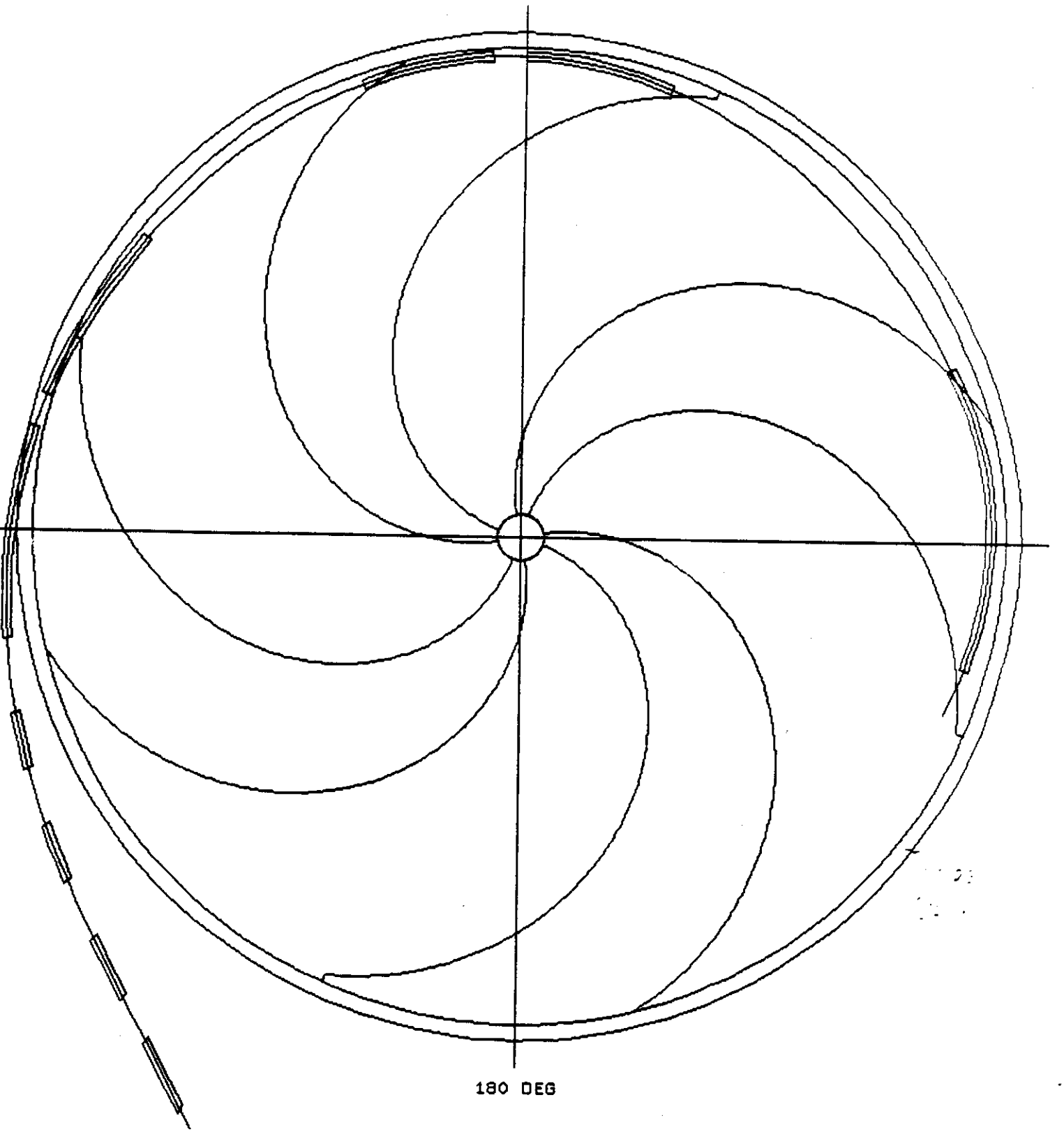

Fig. XVIII. The extraction orbit of one (of a pair of dual) extraction system(s) shown superimposed on the pole tip structure. Boxes superimposed on the extraction orbit represent extraction elements (not to scale). The first two boxes are electrostatic elements and the following boxes are inert magnetic elements.

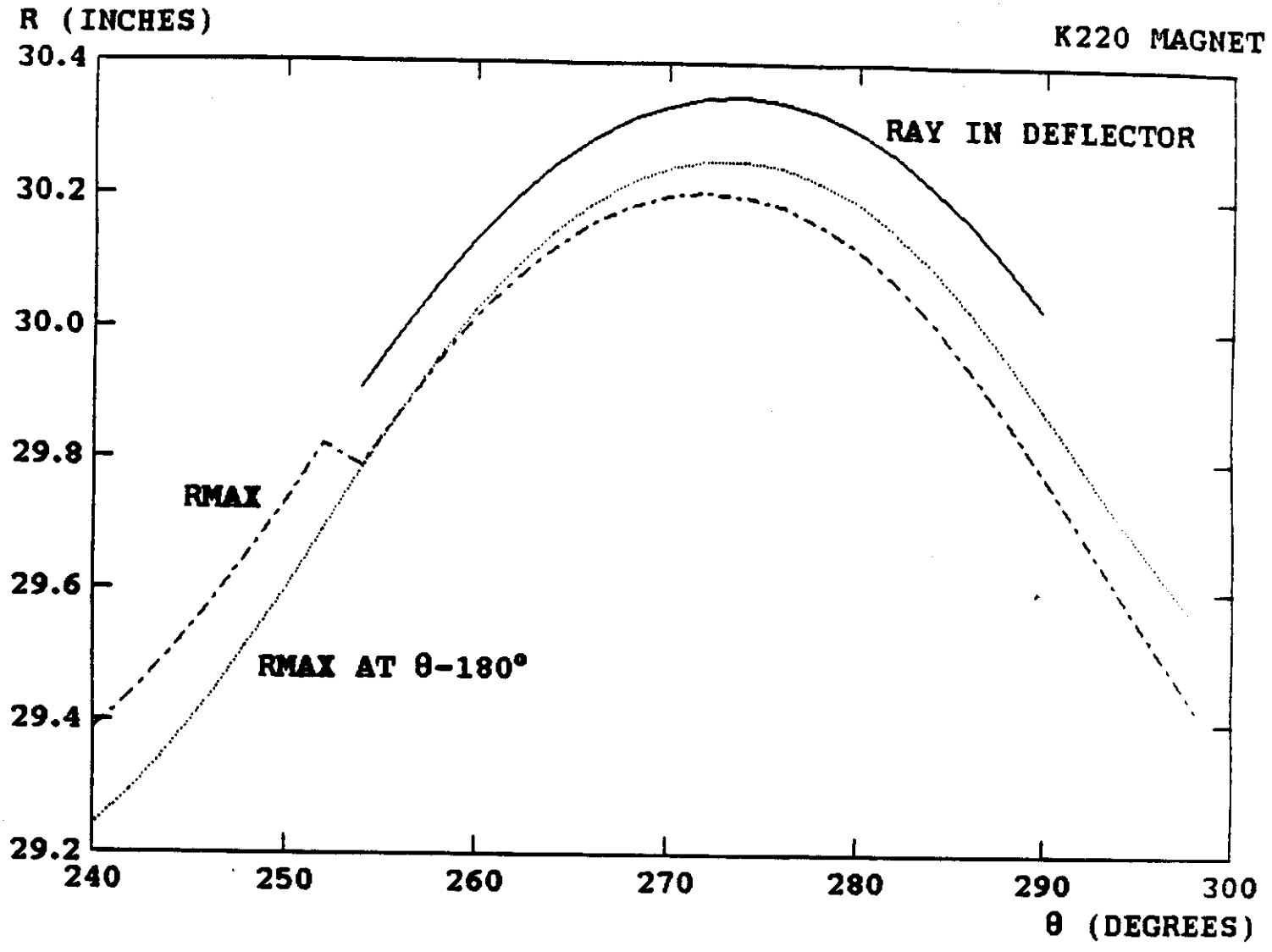

Fig. XIX. A plot showing radius versus azimuth for the extraction trajectory (solid line), the outer envelope of all rays preceding the extraction point (the dot-dash line) and the envelope at an angle 180° earlier (small dots). The clearance between the solid line and both of the earlier orbit postions shows that the family of rays would clear an identical extraction system located 180° away. Selection of the active extraction channel would be accomplished by shifting a small, 0.3 mT, magnetic first harmonic.

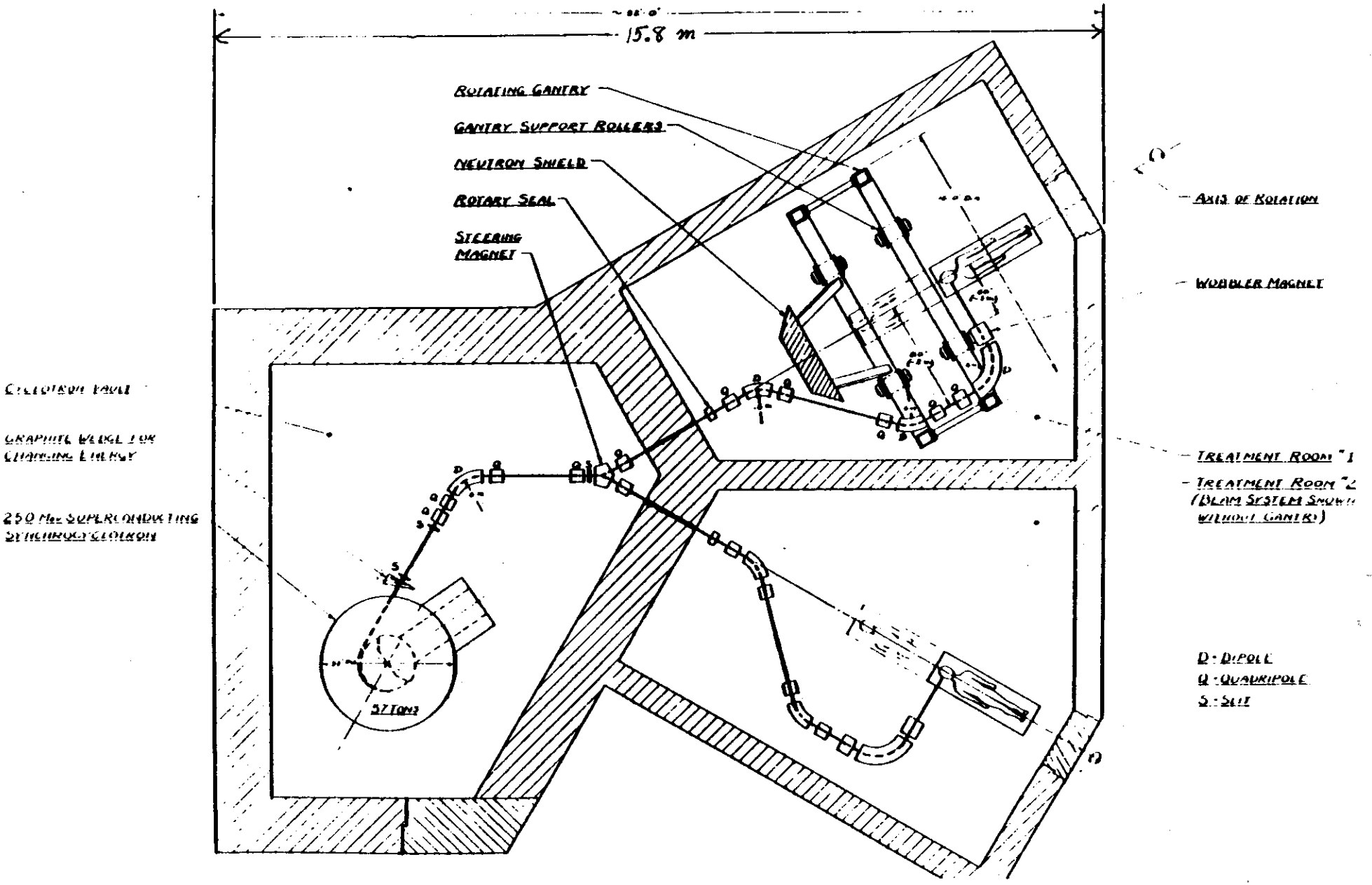

Fig. XX. A possible fan or cluster arrangement for a fixed accelerator. Two gantry-equipped treatment rooms are shown; additional gantry rooms could fan around the cyclotron (i.e. at the top and left in the Figure) giving an arrangement with minimum beam transport lengths to all rooms.

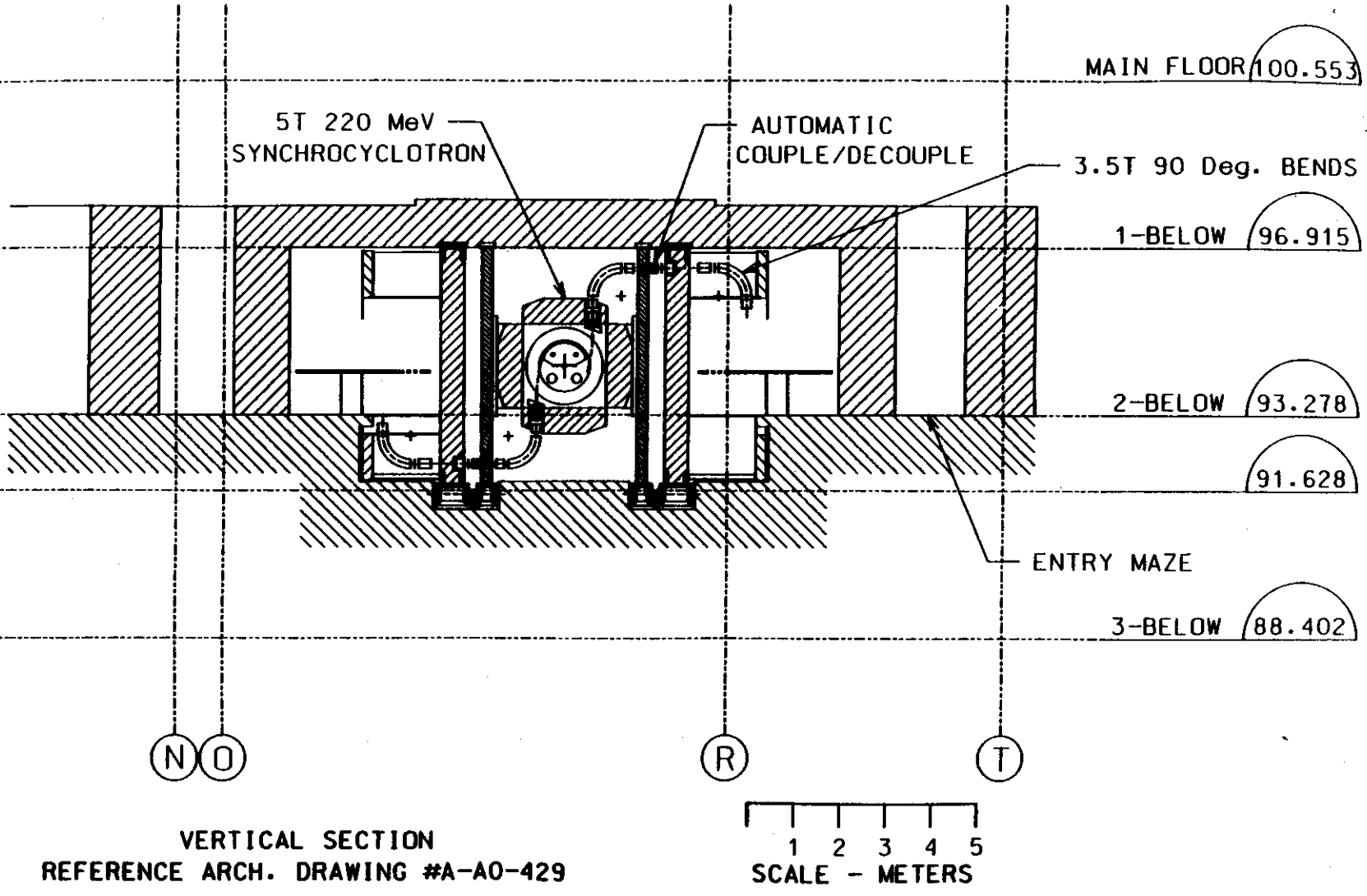

Fig. XXI. A compact, dual beam therapy facility is shown superimposed on the architectural grid of the proposed new Princess Margaret Hospital. The accelerator is a 5 tesla synchrocyclotron with dual extraction. A Sherrill type 3.5T beam transport system (as shown in Figure VIII) guides the beam to each treatment room. The gantry in each room can be decoupled from the cyclotron and prealigned to the patient while a treatment is in process in the opposite room.

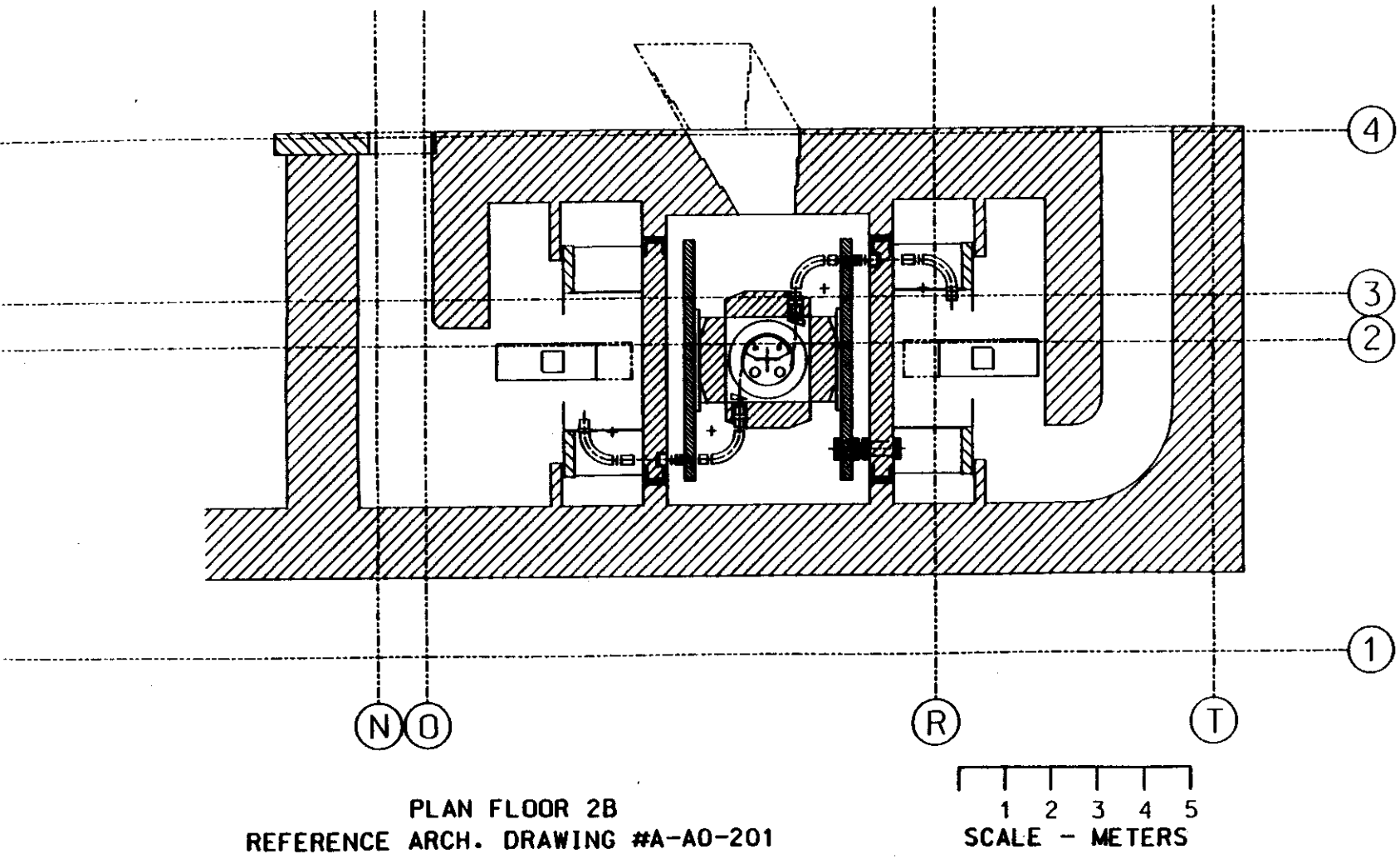

PLAN FLOOR 2B
REFERENCE ARCH. DRAWING #A-AO-201

Fig. XXII. Plan view of the accelerator configuration shown in Fig.XXI. Optional arrangements for entry mazes into the treatment rooms are illustrated on the right and left.

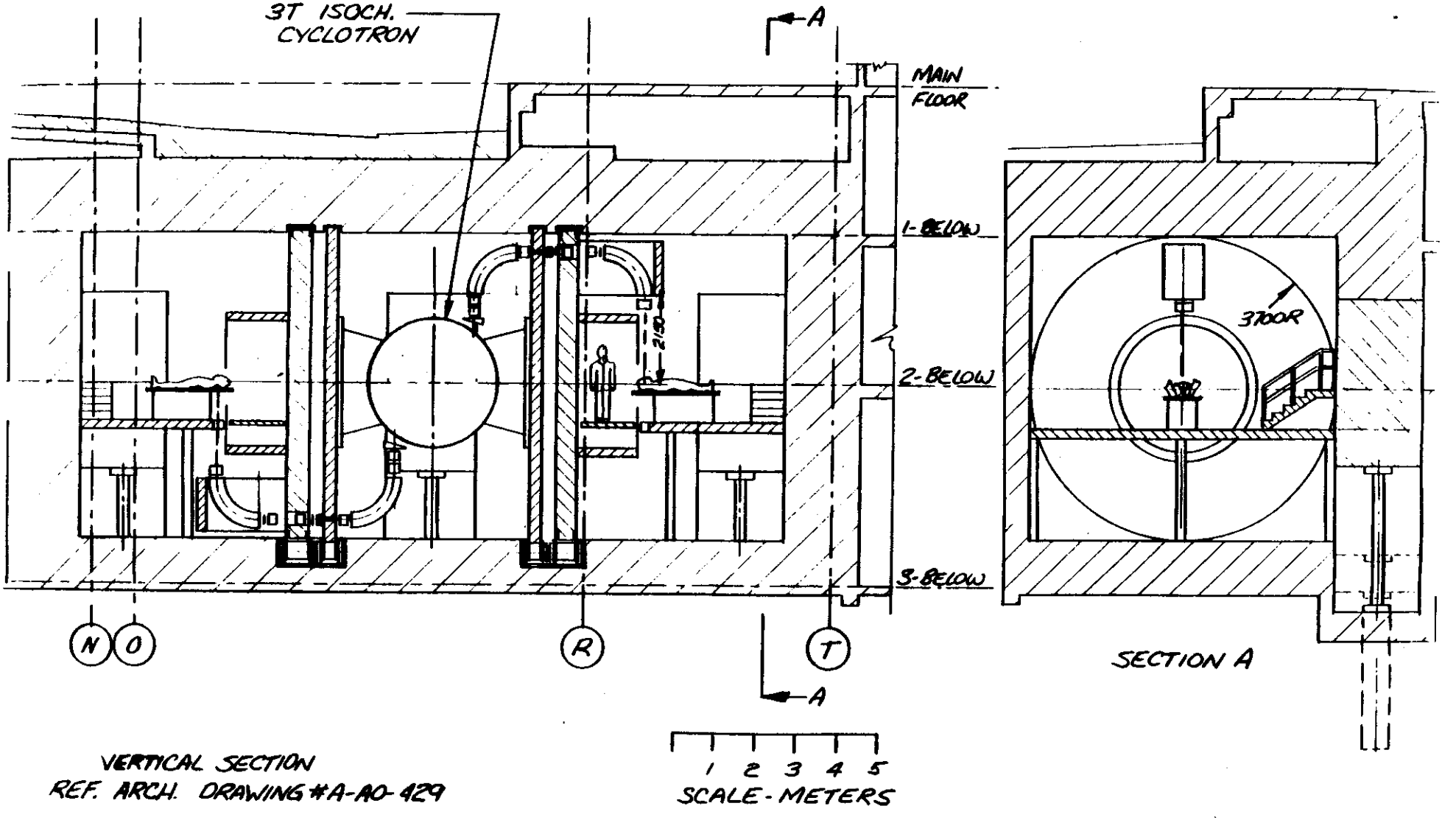

Fig. XXIII. Vertical section view of a 3 tesla isochronous cyclotron superimposed on the architectural grid of the proposed new Princess Margaret Hospital; an end view of the system is at the left. The cyclotron rotates so that all beam bends are in one plane. A field strength in the bending magnets of 2.25 T is required at 220 MeV.

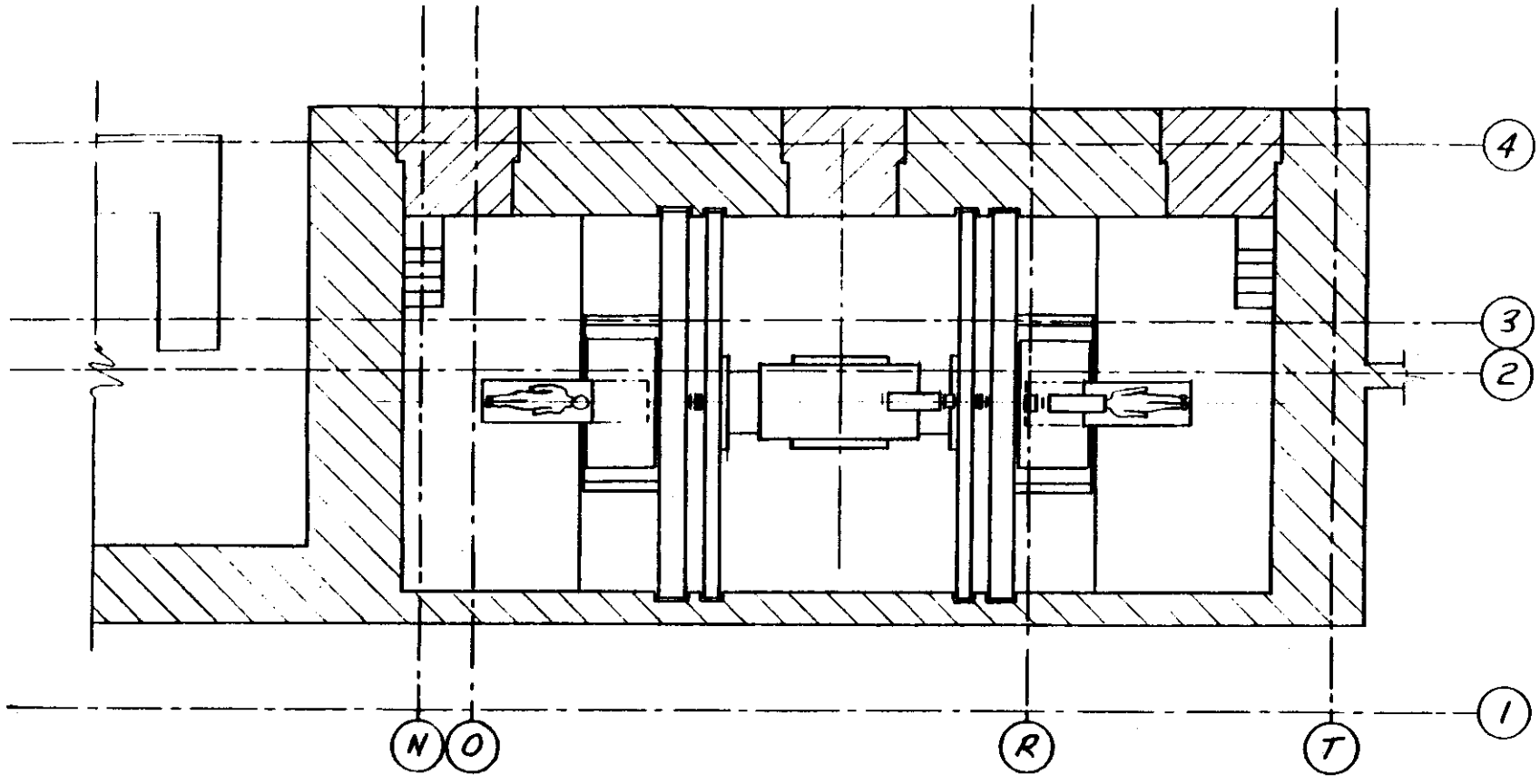

Fig. XXIV. Plan view of the accelerator system shown in Fig. XXIII.

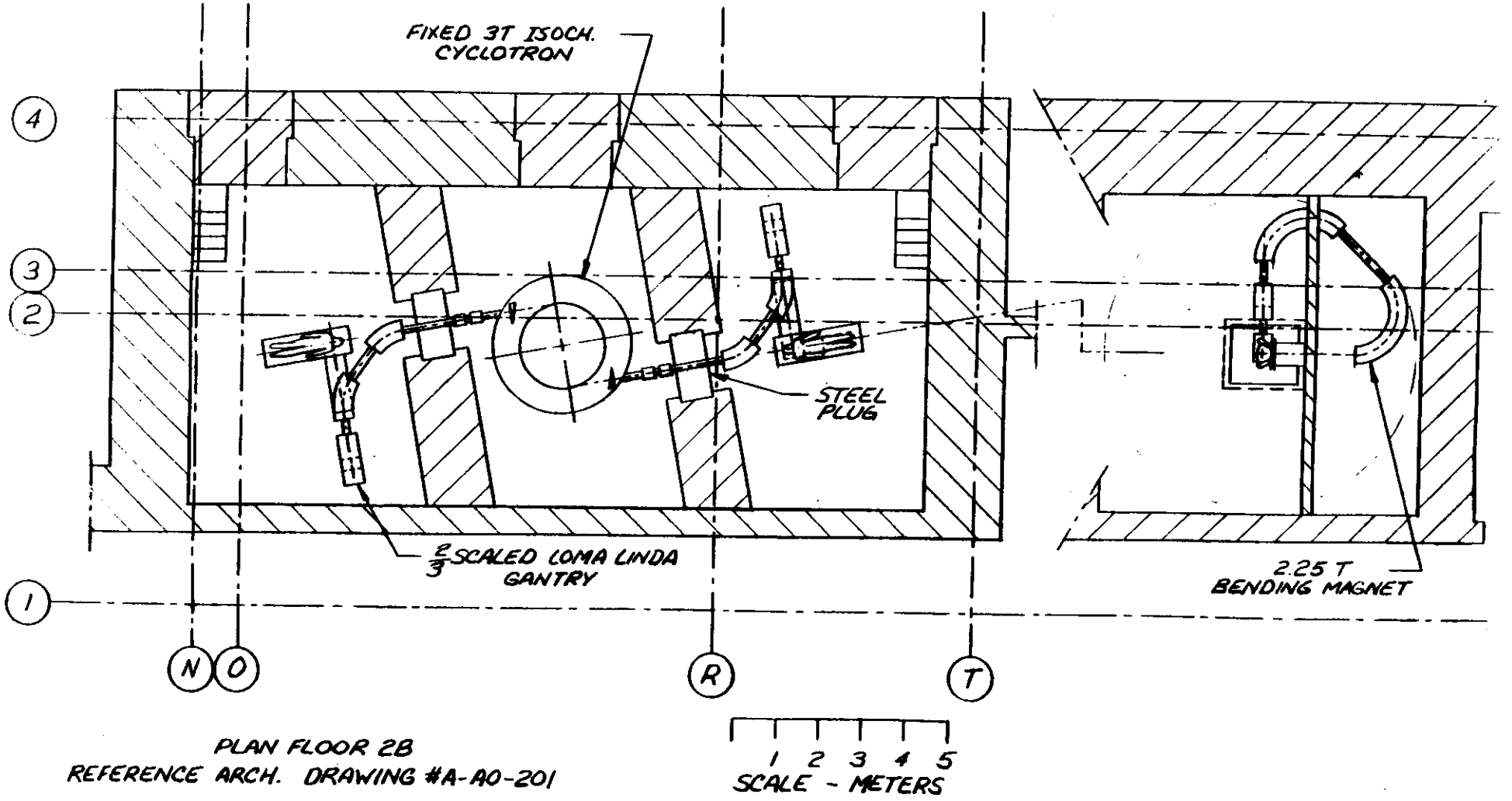

Fig. XXV. A fixed (non-rotating) 3 tesla isochronous cyclotron with dual extraction systems feeding two Loma Linda type gantries. The gantries are scaled by a factor of 3 to 2 relative to Loma Linda and at 220 MeV require 2.25 T fields in the bending magnets.

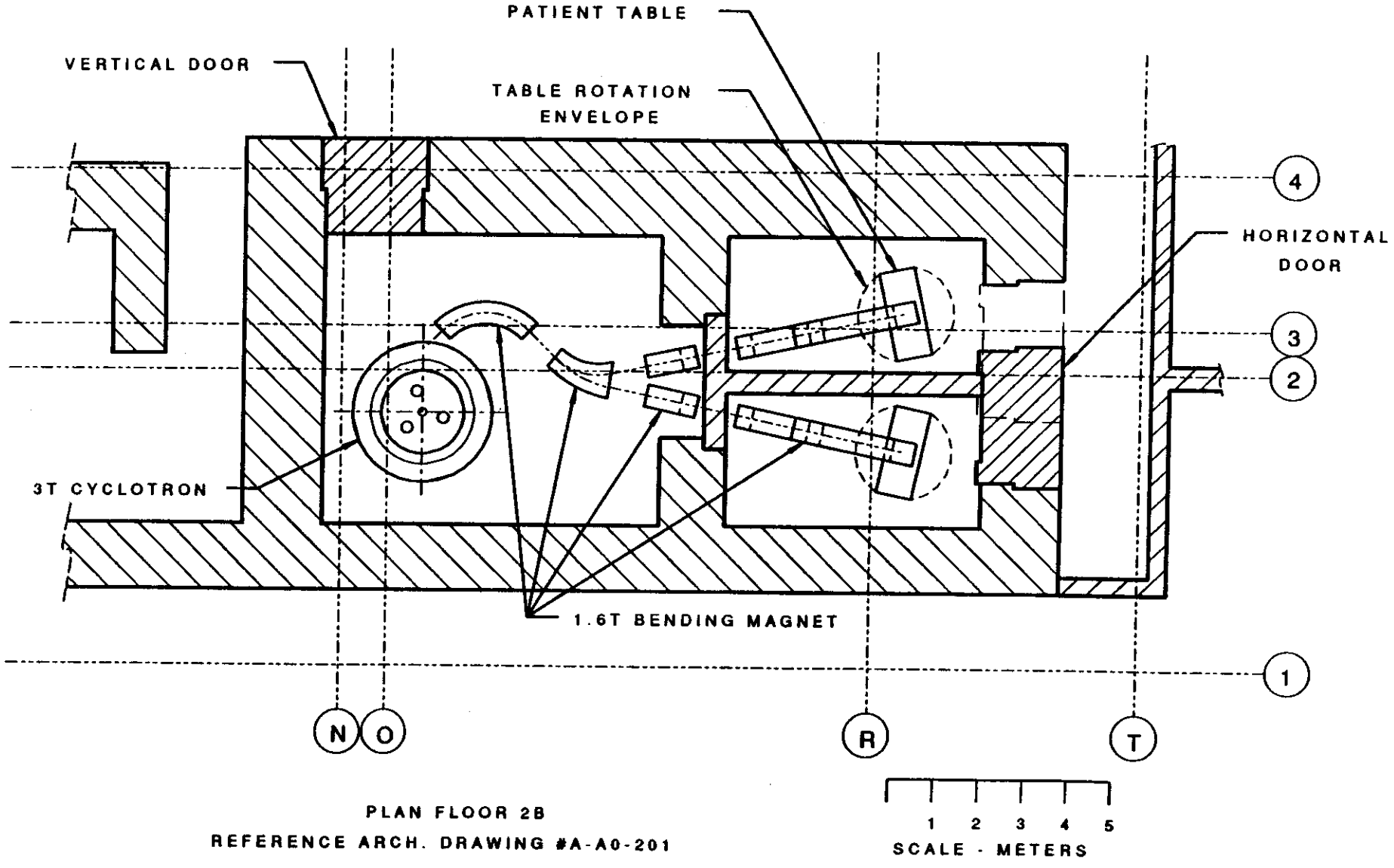

Fig. XXVI. Plan view of a fixed beam therapy system superimposed on the architectural grid of the Princess Margaret Hospital. Beams from any of five fixed angles (see Fig. XXVII) enter either treatment room. A head-to-toe rotation of the patient couch makes the same angles available on the opposite side of the patient without disturbing the position of the patient relative to the couch.

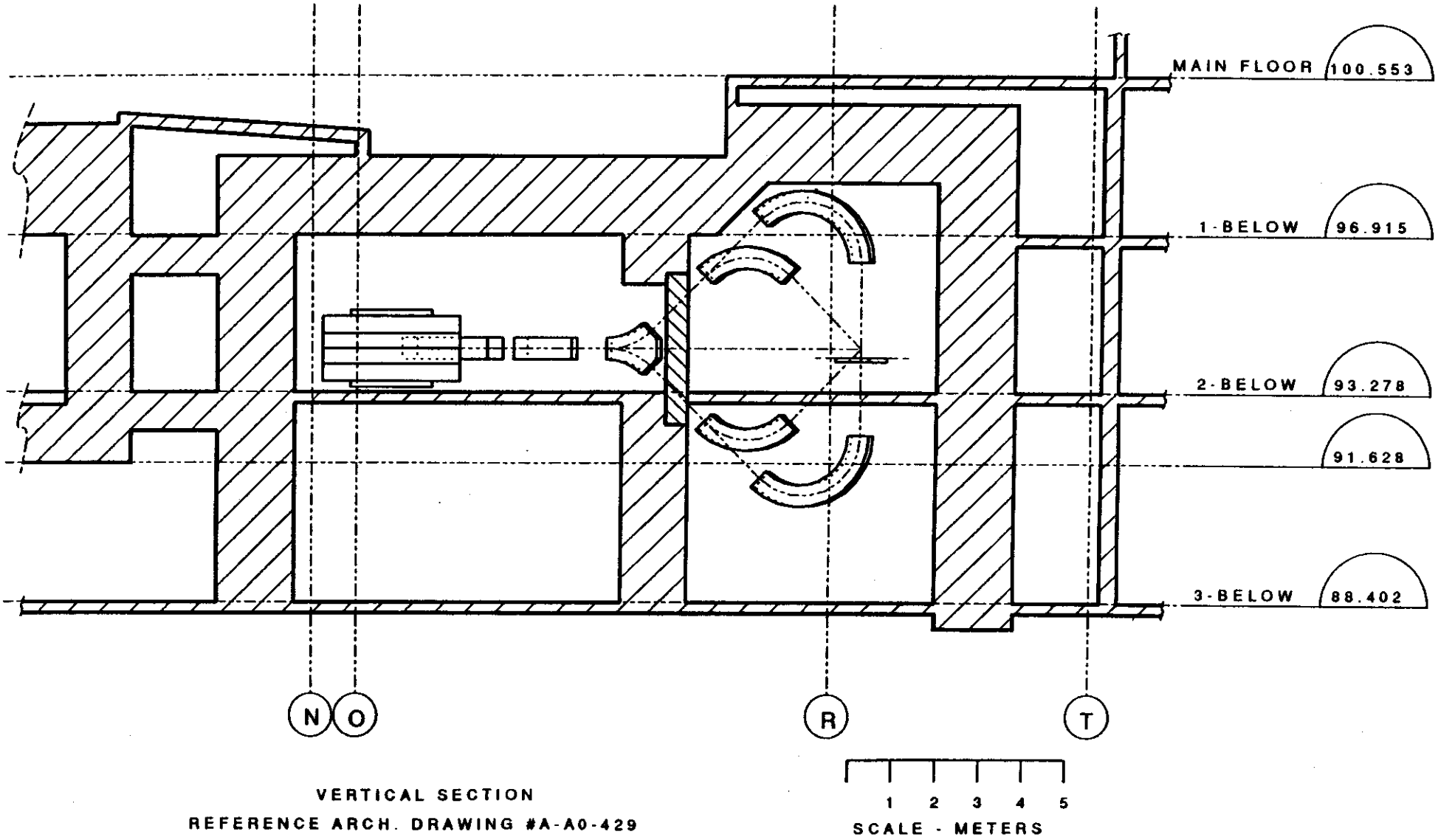

Fig. XXVII. Vertical section view of accelerator arrangement of Fig. XXVI. The cyclotron is at the left; a vertical switching magnet at the center sends the beam straight through or 45° up or down. From each of the 45° lines, 90° and 135° magnets bend the beam back to the patient table to provide treatment ports from above below and at ±45°. A rotation of the patient table in the horizontal plane provides treatments from the opposite side without disturbing patient positioning.

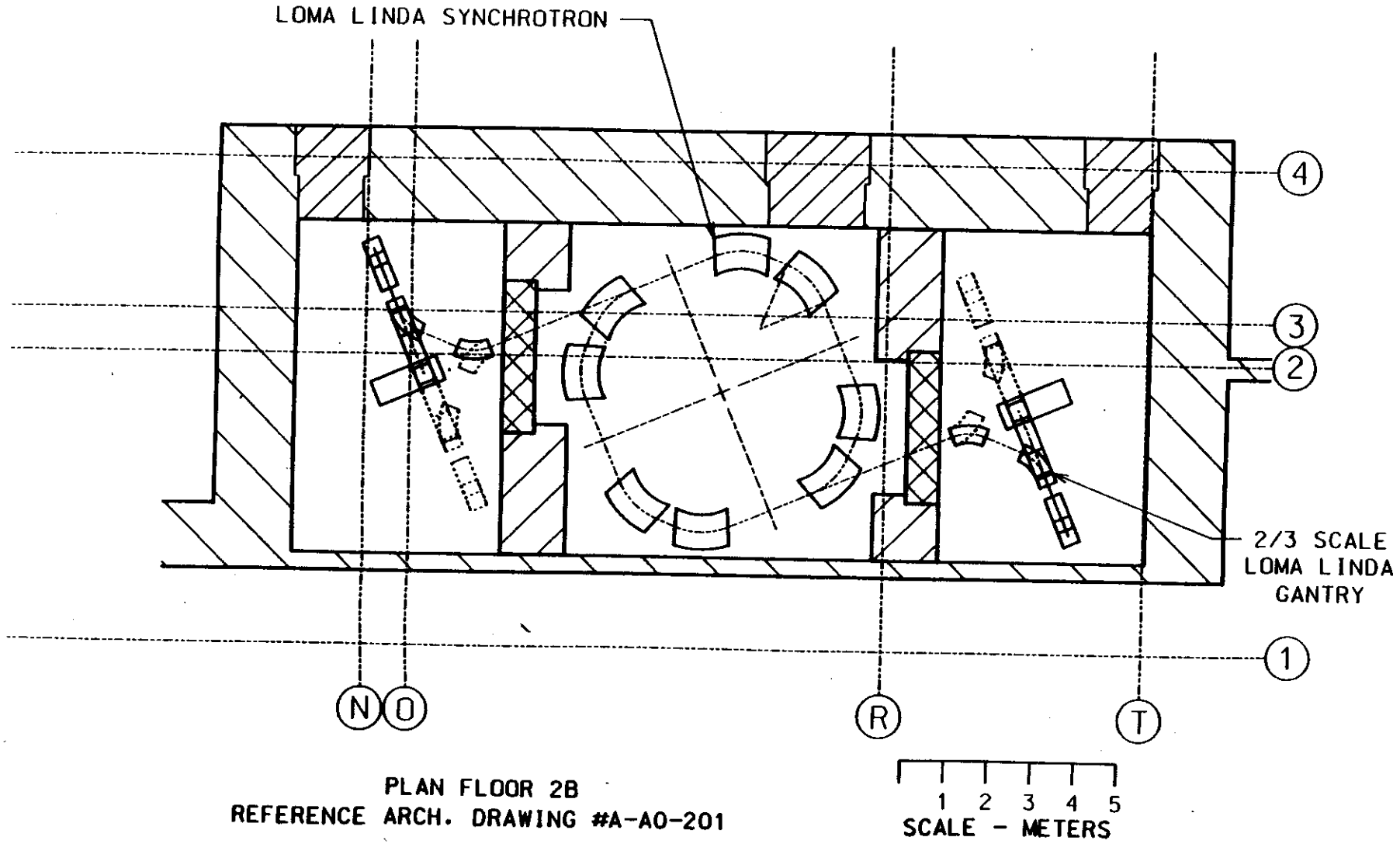

Fig. XXVIII. Plan view showing a Loma Linda sychrotron superimposed on the Princess Margaret Hospital architectural grid and with 3 to 2 scaled Loma Linda gantries at the right and left.

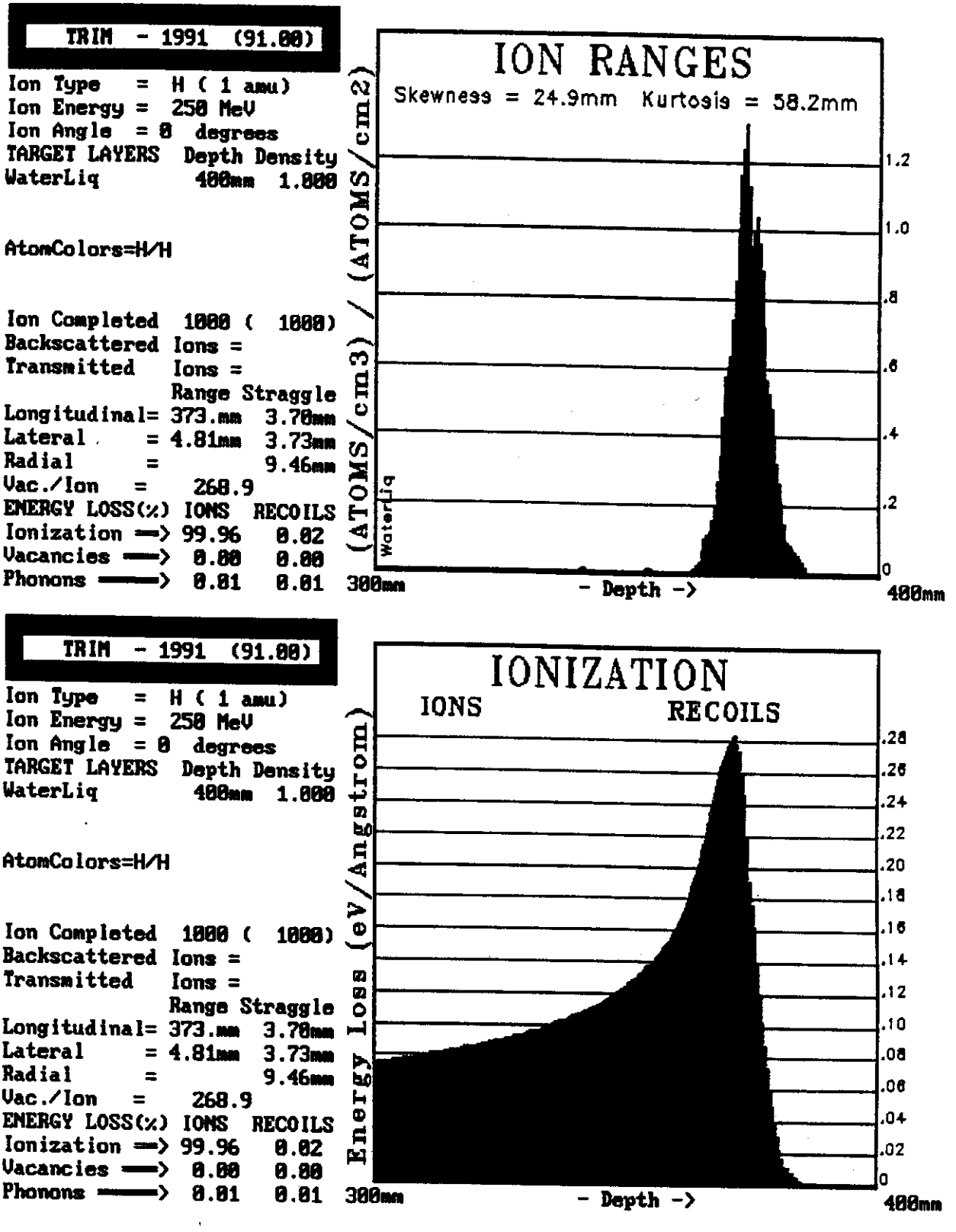

Fig. XXIX. Results of Monte Carlo calculation of range and ionization of 250 MeV particles in water calculated with the program TRIM-91 [20]. A 10 centimeter interval at the end of the range is plotted with the data collected in 1 millimeter bins. The horizontal coordinate is the projection on the x axis of the actual termination point of the calculated ray.

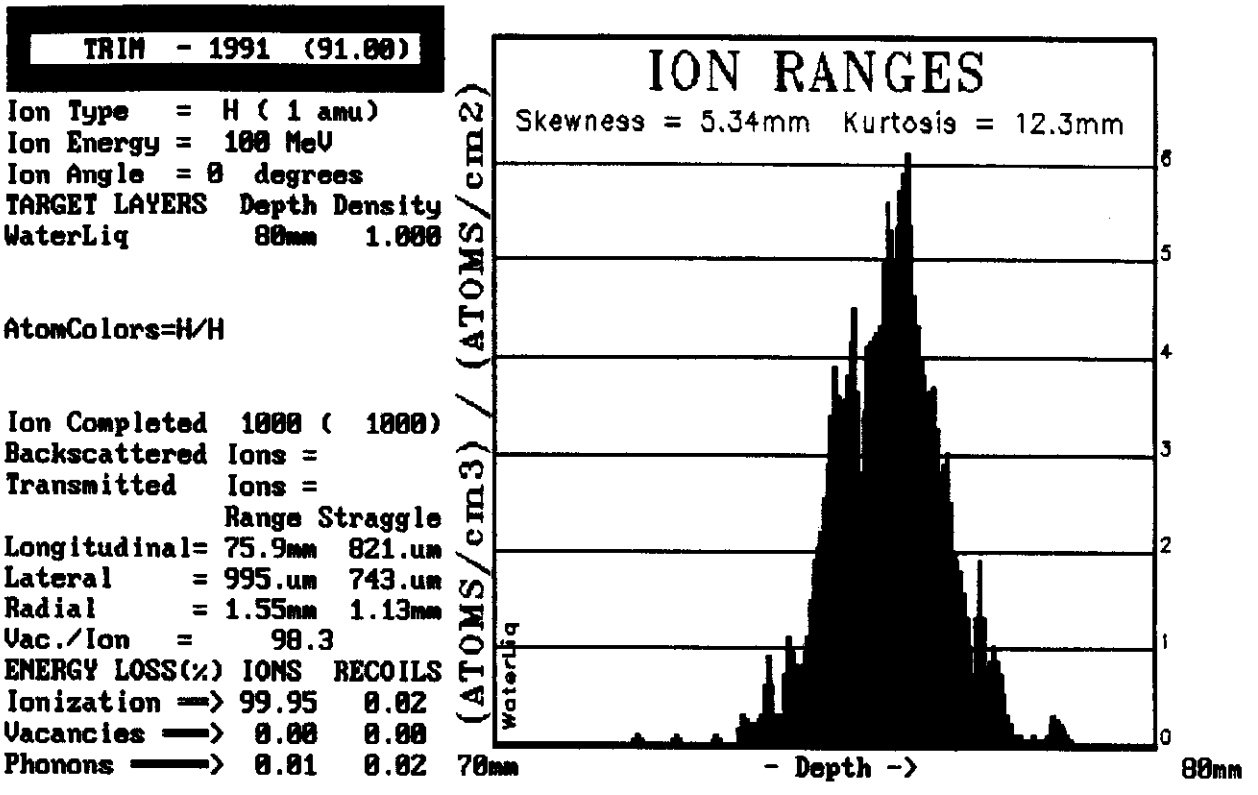

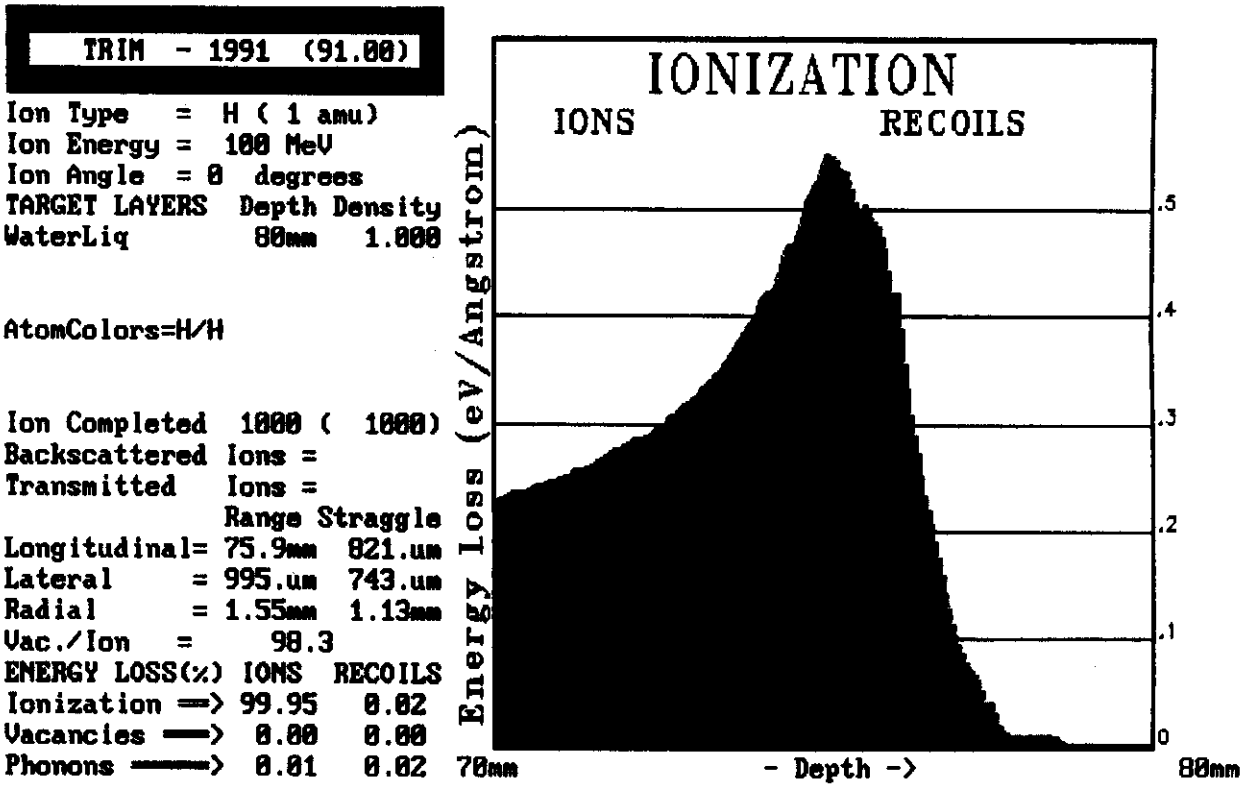

Fig. XXX. Calculations similar to those in Figure XXIX except that the initial energy is 100 MeV and the last 1 centimeter of range is plotted in 0.1 millimeter bins.

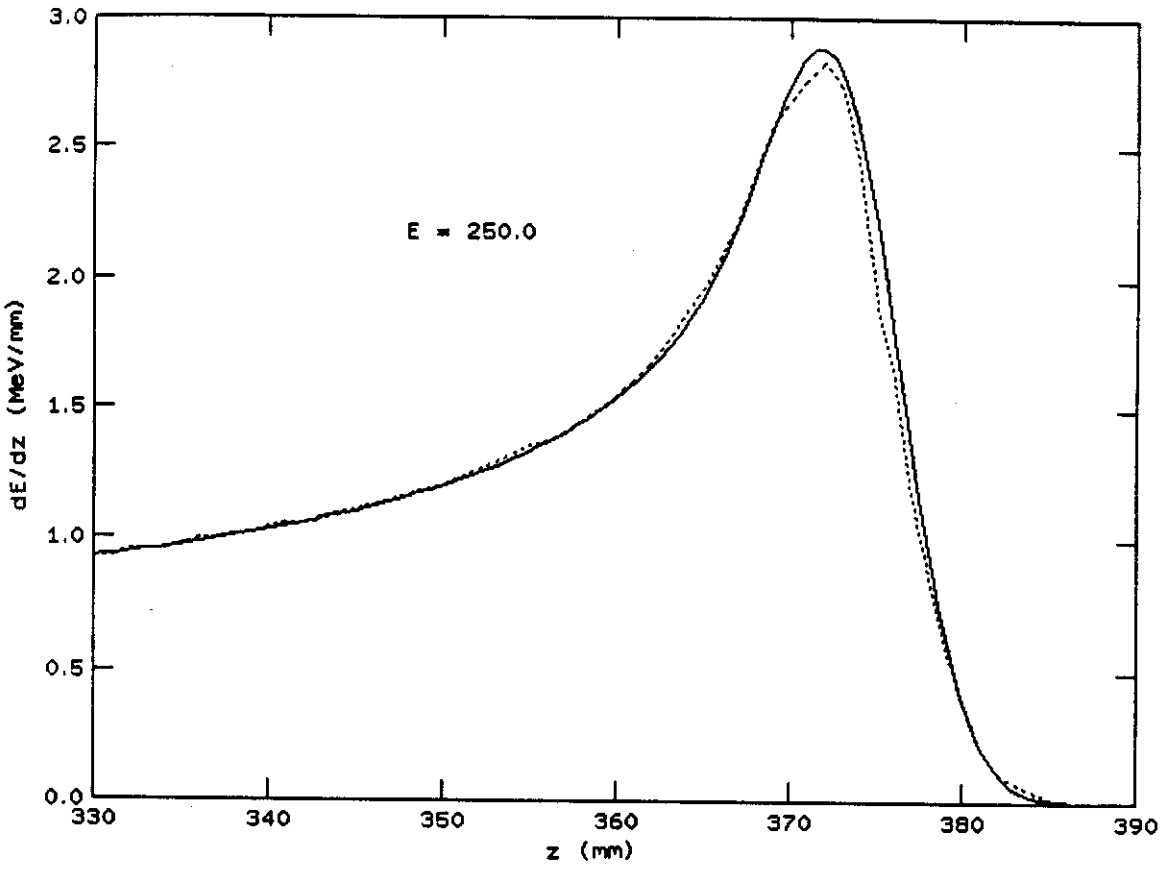

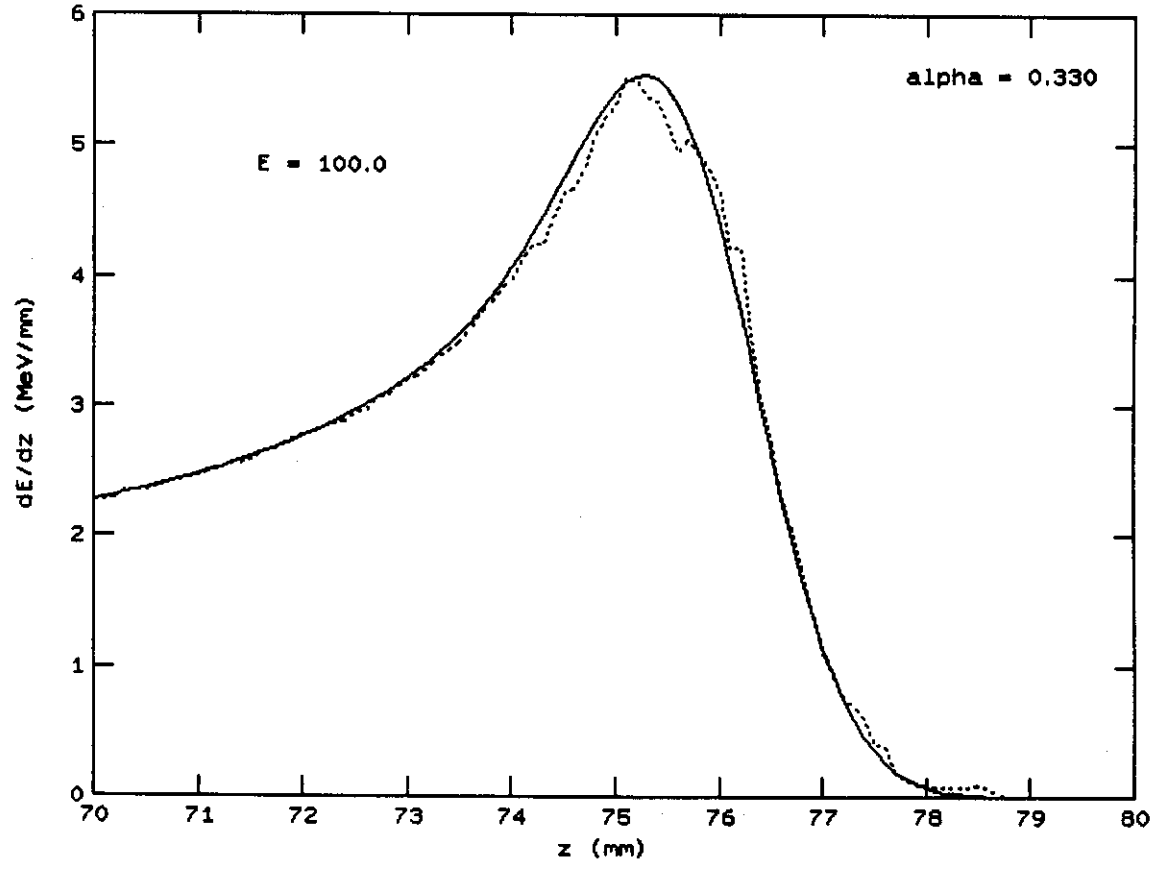

Fig. XXXI. Plots of energy loss at 250 and 100 MeV showing Monte Carlo calculation results from Figures XXIX and XXX (dotted line) vs. an "analytical" calculation (solid line) in which the Bragg curve for a single particle is folded with a Gaussian, with sigma for the Gaussian taken from the calculated longitudinal straggling.